Final report of key comparison CCM.P-K3 absolute pressure measurements in gas from 3×10^{-6} Pa to 9×10^{-4} Pa

D.A. Olson[1], P.J. Abbott[1], K. Jousten[2], F.J. Redgrave[3], P. Mohan[4], S.S. Hong[5]
February 2010

Abstract

This report describes a CCM key comparison of absolute pressure at five National Metrology Institutes (NMIs) that was carried out from August 1998 to May 2002. The goal of the key comparison was to determine the degree of equivalence of NMI standards at pressures in the range of 3×10^{-6} Pa to 9×10^{-4} Pa. The primary standards were dynamic expansion standards at four of the NMIs and a series expansion standard at the fifth NMI. The transfer standard package consisted of two spinning rotor gauges (SRGs) and three Bayard-Alpert ionization gauges. Due to equipment malfunctions, only one of the ionization gauges was calibrated by all of the participants. The SRG measurements were used to compare NMIs at 9×10^{-4} Pa and to normalize the ionization gauge results at that same pressure. The ionization gauge measurements were used to compare NMIs at the lower pressures. The degrees of equivalence of the NMI standards were determined in two ways: deviations from the key comparison reference value (KCRV), and pairwise differences between those deviations. The standards of four of the NMIs show equivalence to the KCRV and each other over the full range of pressures relative to the expanded uncertainties of the comparisons at the k=2 level. The standard of one NMI was equivalent to the KCRV at 3×10^{-6} Pa only, and showed lack of equivalence to the standards of one or more NMIs in the range of 9×10^{-6} Pa to 9×10^{-4} Pa.

[1] NIST: National Institute of Standards and Technology, United States of America
[2] PTB: Physikalisch-Technische Bundesanstalt, Germany
[3] NPL: National Physical Laboratory, United Kingdom
[4] NPLI: National Physical Laboratory of India, India
[5] KRISS: Korea Research Institute of Standards and Science, Republic of Korea

Final report of key comparison CCM.P-K3
absolute pressure measurements in gas from 3×10^{-6} Pa to 9×10^{-4} Pa

Table of Contents

1. Introduction

In May 1996 the Comité Consultatif pour la Masse et les gandeurs apparentéès[6] (CCM) approved proposals by the pressure working groups that identified six comparisons in pressure, the relevant ranges, the transfer standards to be used, and the pilot laboratories. The objective of these comparisons was to ascertain the relative performance of primary pressure standards developed at selected National Metrology Institutes (NMIs). With the signing of the Comité International des Poids et Mesures Mutual Recognition Arrangement (CIPM MRA) [1] by NMIs of Member States of the Metre Convention in October 1999, it was agreed that the six comparisons would serve as *Key Comparisons* under the CIPM MRA. A major objective of the CIPM MRA is to establish the degree of equivalence of national measurement standards maintained by NMIs through key comparisons that test principal measurement methods in the field.

One of the six key comparisons identified was the comparison of vacuum standards over the pressure range of 3×10^{-6} Pa to 9×10^{-4} Pa. The National Institute of Standards and Technology (NIST) was chosen to pilot the comparison. The participants of the comparison were given the option of extending the range down to 3×10^{-7} Pa and up to 9×10^{-3} Pa, although extensions of the range would not necessarily be included in the BIPM (Bureau International des Poids et Mesures) database.

This report summarizes the calibrations of the transfer standards at five NMIs during the period August 1998 to May 2002. The report also summarizes the analysis of the data, the calculation of uncertainties, the proposal for a Key Comparison Reference Value (KCRV), and the degrees of equivalence. The participating NMIs were NIST (USA, pilot laboratory), PTB (Germany), NPL (United Kingdom), NPLI (India), and KRISS (Korea). A sixth NMI, the Istituto di Metrologia "G. Colonnetti" (IMGC, Italy), took part initially but withdrew their results prior to the circulation of Draft A[7]. The transfer standard package initially consisted of three hot-cathode ionization gauges and two spinning rotor gauges. The ionization (ion) gauges were calibrated over the full pressure range, and the spinning rotor gauges were calibrated at 9×10^{-4} Pa. Only one of the ionization gauges was calibrated by all the participants due to difficulties described later. Results of this ion gauge for each NMI at 9×10^{-4} Pa were normalized to the results of the spinning rotor gauges at the same pressure to correct for pressure-independent shifts in the ion gauge characteristics.

2. Primary standards

Two types of primary standards were used as the principal pressure measurement methods for this comparison: (1) dynamic or continuous expansion standards were used at KRISS, NIST, NPLI, and PTB; (2) a series (also called static) expansion standard was used by NPL.

[6] Consultative Committee for Mass and related quantities.
[7] Since January 1, 2006, IMGC is now known as Istituto Nazionale di Ricerca Metrologica (INRIM).

2.1 Dynamic expansion standard at NIST

In a dynamic expansion standard, pressures are generated by producing a known flow of gas which passes through an orifice of known conductance, thereby producing a known pressure drop across the orifice. The NIST ultra high vacuum (UHV) standard was used to calibrate the gauges in this comparison [2]. The standard consists of two main elements: a low-range flowmeter, and a vacuum chamber where the instruments are mounted for calibration. The full calibration range of the standard is 10^{-7} Pa to 10^{-1} Pa. The vacuum chamber is approximately 45 cm in diameter and 110 cm long with a total volume of approximately 180 L. The chamber is evacuated with a turbomolecular pump. A partition separates the chamber into two approximately equal volumes. The upper and lower chambers normally communicate through a 1.1 cm diameter orifice. The orifice is mounted in a plate that is attached to a lifting mechanism. When the orifice plate is in the raised position, the upper and lower chambers communicate through a 13 cm diameter hole that allows a larger effective pumping speed for evacuating the upper chamber. When the orifice plate is lowered into place, it seals against a liquid gallium-indium alloy that fills a groove in the partition.

2.2 Dynamic expansion standard at PTB

The primary standard at PTB is a continuous expansion system, called CE3 [3], with its flowmeter FM3 [4]. Known gas flow is injected into a flow divider chamber, which then flows into either a UHV chamber through a larger conductance orifice or into a XHV (extreme high vacuum) chamber through a smaller conductance orifice with about 1/100 of the conductance to the UHV chamber. The XHV and UHV chambers are each evacuated with cryo condensation pumps through pump orifices of similar conductances; when both pumps are operating the generated pressure in the XHV chamber is about a factor of 100 lower than that in the UHV chamber. For the present comparison, only the pressure generated in the UHV chamber was used while the XHV chamber was pumped by a turbomolecular pump. This only slightly increased the uncertainty of the generated pressure.

After the measurements were taken for this comparison, the system was completely reviewed in 2005 and 2008 and a few errors of different significance were found. The most significant was the discovery of a virtual leak in the working volume of FM3 that falsified the measurement of the conductance. The leak was immediately redressed. Also it was found that the small orifice C_{02} [3] (nominal diameter 700 µm) from the flow divider into the XHV chamber was dented and had changed its dimension, probably due to a high differential pressure during a pump down process after venting. The conductance was re-measured. Other errors (mainly software implementation) did not significantly affect the PTB results of the comparison.

2.3 Series expansion standard at NPL

The calibrations at NPL were performed on the high-vacuum series expansion apparatus (SEA I/II). Using the apparatus, calculable pressures between 5×10^{-7} Pa and 9×10^{2} Pa

may be generated using the series expansion method. A sample of gas is trapped in one of four small vessels and then expanded sequentially into large and small vessels, which have previously been evacuated to a low pressure. This procedure is repeated using subsequent expansion stages until the gas is expanded into the calibration vessel. The pressure of the initial gas sample is measured using a calibrated quartz Bourdon tube gauge. By varying the initial pressure and the number of stages of expansion, a range of pressures may be generated in the calibration vessel. Using this apparatus, up to four stages of expansion are employed. The pressure generated is calculated from knowledge of the initial pressure, the ratio of the volumes, and the gas temperatures [5].

2.4 Dynamic expansion standard at NPLI

The NPLI dynamic expansion standard is an orifice flow system that consists of two 30 cm diameter spheres with an orifice mounted in the connection between the spheres [6, 7]. Gas flow to the spheres is measured by a constant volume flowmeter, which makes use of a spinning rotor gauge and a 13 Pa full scale (absolute) capacitance diaphragm gauge to measure the rate of rise of pressure in the flowmeter volume which is nominally 0.13 liter. The chambers are evacuated with a turbomolecular drag pump backed by a diaphragm pump. A titanium sublimation pump connected to the lower of the two chambers allows reaching base pressures on the order of 10^{-8} Pa.

2.5 Dynamic expansion standard at KRISS

The primary standard for ultra high vacuum (UHV) at KRISS used for this comparison is an orifice type dynamic expansion system. It consists of two dynamic calibration systems: one for high vacuum (HV) from 10^{-5} Pa to 10^{-2} Pa, and the second for UHV from 10^{-7} Pa to 10^{-5} Pa. The UHV system is connected to the HV by a porous plug having a very small conductance (6.36×10^{-3} L/s in nitrogen at 23 ºC). Gas is supplied to the high vacuum system from a constant pressure-type flowmeter, some of which flows through the porous plug into the UHV chamber. The HV system is evacuated using a turbomolecular pump with a pumping speed for nitrogen of 345 L/s, and the UHV system is evacuated using a closed loop helium refrigerator-type cryopump with a pumping speed for nitrogen of 1500 L/s. Further details of the systems and a full uncertainty analysis are given in [8].

3. Transfer standards

The transfer standard package consisted initially of two spinning rotor gauges (SRG-027 and SRG-030) and three ionization gauges (BA-16, BA-17, and SI-404). Table 1 lists characteristics of the gauges and controllers that were supplied with the package. Listed also is a fourth ionization gauge (BA-19) that replaced gauge BA-17 when it failed en route. Ionization gauges BA-16, BA-17, and the replacement BA-19 were of the twin-

Table 1. Transfer standards used in CCM.P-K3.

Gauge Identifier	Pressure Range for Calibration / Pa	Gauge Description	Controller	Comments
SRG-027	$9x10^{-4}$	Spinning rotor gauge, 4.76 mm diameter chrome-steel rotor	None provided	Thimble T27
SRG-030	$9x10^{-4}$	Spinning rotor gauge, 4.76 mm diameter chrome-steel rotor	None provided	Thimble T18
SI-404	$3x10^{-6}$ to $9x10^{-4}$	Metal enclosed Bayard-Alpert ionization gauge ('Stabil-Ion' gauge)	Granville-Phillips model 360 ion gauge controller, Ch. IG2	
BA-16	$3x10^{-6}$ to $9x10^{-4}$	Glass enclosed, Bayard-Alpert ionization gauge with opposed twin tungsten filaments	Granville-Phillips model 303 ion gauge controller, Ch. 1	
BA-17	$3x10^{-6}$ to $9x10^{-4}$	Glass enclosed, Bayard-Alpert ionization gauge with opposed twin tungsten filaments	Granville-Phillips model 303 ion gauge controller, Ch. 2	Filament detached, IMGC to NIST
BA-19	$3x10^{-6}$ to $9x10^{-4}$	Glass enclosed, Bayard-Alpert ionization gauge with opposed twin tungsten filaments	Granville-Phillips model 303 ion gauge controller, Ch. 2	*Replacement for BA-17*. Filament detached, NIST to KRISS

tungsten filament, glass-envelope tube, Bayard-Albert[8] gauge type. SI-404 was a metal-enclosed gauge tube or "Stabil-Ion" Bayard-Albert gauge type. All of the ionization gauges were calibrated as a unit (controller + cable + electrical box + gauge tube). A Fluke Model 7911 multimeter was supplied to measure the bias voltages. Ionization vacuum gauges are relatively unstable transfer gauges, and multiple gauges provided redundancy for gauge response shifts and failure of the units. Pilot laboratory experience with repeat customer calibrations (after shipment) of glass-envelope tube ionization gauges using twin-tungsten filaments showed average response shifts of the order of 3 % [9]. Prior to the comparison, repeat calibrations by the pilot laboratory on the Stabil-Ion gauge (SI-404) showed stability on the order of 1 %. The effect of shipment on response shifts was not known.

[8] Certain commercial equipment, instruments, or materials are identified in this paper to foster understanding. Such identification does not imply endorsement by NIST nor does it imply that the equipment or materials are necessarily the best for the purpose.

The two spinning rotor gauges used chrome-steel rotors of 4.76 mm nominal diameter. The rotors were supplied with specific thimbles for their operation that accepted either MKS-type or LH-type suspension heads. Neither suspension heads nor SRG controllers were supplied with the transfer package. The long-term stability of SRG rotors is typically 1 % or better [10], and one of the two rotors for which the pilot laboratory had repeat data showed a stability of 0.2 % over an 18 month period. Due to the superior calibration stability of the SRGs, they were used to normalize the ionization gauge data at the highest calibration pressure, an approach that was also used in an earlier comparison of vacuum standards by several of the participants [11].

4. Organization of the key comparison

4.1 Chronology of the measurements

The chronology of calibrations during the measurement phase of the comparison is listed in Table 2. After initial measurements at NIST, the transfer standard package was circulated to the European region, with two sets of measurements at PTB. After returning to NIST it was sent to NPLI, returned to NIST, was sent to KRISS, and returned to NIST. The total time to complete the measurement phase was 3 years and 9 months, which was 13 months longer than proposed in the protocol. In total, NIST made four sets of measurements on the transfer standards. In the nomenclature given in Sec. 6, each instance in which NIST and PTB calibrated the package is denoted as a cycle (PTB had 2 cycles, NIST had 4 cycles).

4.2 Problems during the comparison

Several equipment malfunction problems were encountered during the comparison. During the shipment of the package from IMGC to NIST in November 1999, the filament on BA-17 detached. It was replaced at NIST with BA-19, which NIST used in the January 2000 calibration. En route from NIST to KRISS in August of 2001, the filament on BA-19 detached. The controller used for the glass enclosed ionization gauges failed at KRISS, so KRISS was only able to make measurements on ionization gauge SI-404. Prior to the final NIST calibration, the ionization gauge controller was repaired and NIST calibrated BA-16. All participants calibrated both spinning rotor gauges, however the only ionization gauge calibrated by all participants was SI-404. The functioning gauges tested by each participant are listed in Table 2.

5. General calibration procedure

The transfer standards were calibrated at the participant's vacuum standards using high purity natural isotopic argon with a minimum purity of 99.999 %. The procedure to be followed included methods for mounting the gauges, pre-test to verify operation, bake-out of the gauges installed in the vacuum standards, pre-conditioning, as well as the calibration itself.

Table 2. Chronology of the measurements and gauges calibrated for each cycle of each NMI participant.

NMI *j* cycle *m*	Start Date	End Date	Gauges Calibrated				
			SRG-027 SRG-030	SI-404	BA-16	BA-17	BA-19
NIST1	11-Aug-1998	18-Sep-1998	yes	yes	yes	yes	
PTB1	25-Feb-1999	4-Mar-1999	yes	yes	yes	yes	
NPL	20-Apr-1999	26-Apr-1999	yes	yes	yes	yes	
PTB2	9-Jun-1999	14-Jun-1999	yes	yes	yes	yes	
IMGC	14-Sep-1999	Withdrew data	yes	yes	yes	yes	
NIST2	6-Jan-2000	27-Jan-2000	yes	yes	yes		yes
NPLI	7-Jun-2000	12-Jul-2000	yes	yes	yes		yes
NIST3	13-Dec-2000	13-Feb-2001	yes	yes	yes		yes
KRISS	16-Nov-2001	21-Nov-2001	yes	yes			
NIST4	23-Apr-2002	2-May-2002	yes	yes	yes		

5.1 Preparation for calibration

The three ionization gauges were mounted with their filaments oriented vertically. For the two glass envelope gauges, the controller cables were connected for operation with the "right-hand" filament, and the "left-hand" filament was not used. The connector cable for the Stabil-Ion gauge was keyed to provide proper filament operation. The SRG gauge heads were also mounted vertically with the thimble assembly horizontal. Following the installation of the transfer standards, the vacuum chambers were evacuated to a pressure below 1×10^{-4} Pa and the operation of the gauges was verified. This included suspending and "spinning up" the SRG rotors. The sensitivity and emission current parameters in the ion gauge controllers, and the operating parameters in the SRG controllers, were verified or set to the values specified in the protocol.

Participants baked the vacuum standards with the transfer standards installed and power to the ionization gauges, to at least 150 ºC using their normal baking procedure. Teflon-insulated bake cables were provided with the transfer standards for use during the bake-out. Following bake-out the system was allowed to cool and the Teflon-insulated bake cables were replaced with the standard-operation cables. The SRG rotors were re-suspended and operated for at least eight hours to reach equilibrium. Prior to calibration, the gauges were operated at an elevated argon pressure of 1×10^{-2} Pa for one hour, and then the vacuum standards were re-evacuated to base pressure.

5.2 Calibration of the gauges

The ionization gauges were calibrated in argon at six increasing target pressure steps at the values 3×10^{-6} Pa, 9×10^{-6} Pa, 3×10^{-5} Pa, 9×10^{-5} Pa, 3×10^{-4} Pa, and 9×10^{-4} Pa. Participants had the option of calibrating at 3×10^{-7} Pa and 9×10^{-7} Pa if their vacuum standard could achieve those pressures. The *calibration run* of the six pressures was to be achieved in a single day, however this was not accomplished for all runs of all participants. Each pressure was to be generated a minimum of three times in the calibration run. The entire run was repeated on at least one separate day. The spinning rotor gauges were calibrated at 9×10^{-4} Pa. Optional calibrations for the SRGs were at 3×10^{-3} Pa and 9×10^{-3} Pa. There was no requirement for how close the measured/generated pressure of the primary standard was to the target pressure.

Prior to introducing the calibration gas for each calibration run, the base pressure of the vacuum standard, P_0, was measured along with gauge reading at the base pressure, p_{G0}.[9] For static expansion systems this was done prior to every expansion; for orifice flow systems this was done prior to the establishment of gas flow. For either method, sufficient data was taken to ensure that equilibrium had been reached.

Tables 3 and 4 summarize the calibration measurements made by each participant for the spinning rotor gauges and ionization gauge SI-404, respectively. As can be seen, the number of calibration runs and number of points per pressure step was not the same for all the participants. Only NPL calibrated the ion gauges at 9×10^{-7} Pa; both PTB and NPL calibrated the SRGs at pressures greater than 9×10^{-4} Pa. For the second PTB calibration cycle (PTB2), the SRG data was mistakenly not taken at 9×10^{-4} Pa. Their results at 2.8×10^{-3} Pa and 8.2×10^{-3} Pa showed no pressure dependence for the accommodation coefficient, so values obtained at the higher pressure were used in place of a result at 9×10^{-4} Pa. The ion gauge calibration runs at NPLI and the third NIST calibration (NIST3) spanned more than one day. In analyzing the results, all the data provided by each participant was used in characterizing the transfer standards, the reference value, and the degree of equivalence of the comparison. Table 5 lists the electrical parameters of ionization gauge SI-404 that were taken at the beginning of the day, prior to the start of the calibration run, for each NMI. If a calibration run spanned multiple days, the parameters listed are for the start of each day. Listed are the grid bias voltage, the filament bias voltage, and the voltage drop across the grid-line resistor (1 kΩ). As can be seen, the gauge performed consistently with regard to the electrical parameters for all cycles at all NMIs.

6. Reduction and analysis of the reported data

The reduction and analysis of the key comparison data required several factors to be addressed. These included zero-pressure effects, temperature-dependent sensitivities of

[9] All upper-case "*P*" letters refer to a pressure of the primary standard at the NMIs, either a measured pressure or a target pressure. All lower-case "*p*" letters refer to a pressure indication of the transfer standard gauges.

Table 3. Summary of conditions for the spinning rotor gauge calibrations.

NMI j cycle m	SRG-027, i = 1			SRG-030, i = 2		
	Number calibration runs	Number points per run	Number of points N_{1jm}	Number calibration runs	Number points per run	Number of points N_{2jm}
NIST1	8	1 to 5	19	5	2 to 5	14
PTB1	3	3	9	3	3	9
NPL	6	3	18	6	3	18
PTB2[1]	2	6	12	2	6	12
NIST2	6	1 to 2	11	6	1 to 2	11
NPLI	7	1 to 4	16	7	1 to 4	16
NIST3	5	2	10	5	2	10
KRISS	3	4	12	3	4	12
NIST4	4	2 to 3	9	4	2 to 3	9

Notes:
1. PTB2 data taken at 2.8×10^{-3} Pa and 8.2×10^{-3} Pa rather than 9.0×10^{-4} Pa.

Table 4. Summary of conditions for the ionization gauge calibrations using SI-404. Bold lettering indicates measurements outside required range.

NMI j cycle m	Number calibration runs	Number points per pressure	Pressure Range / Pa		Number points $3\text{x}10^{-6}$ Pa to $9\text{x}10^{-4}$ Pa
			Low	High	
NIST1	7	1 to 2	$3.0\text{x}10^{-6}$	$9.0\text{x}10^{-4}$	73
PTB1	3	3	$3.0\text{x}10^{-6}$	**$9.0\text{x}10^{-3}$**	54
NPL	2	3	**$9.0\text{x}10^{-7}$**	$9.0\text{x}10^{-4}$	36
PTB2	2	3	$3.0\text{x}10^{-6}$	**$9.0\text{x}10^{-3}$**	35
NIST2	5	2 to 3	$3.0\text{x}10^{-6}$	$9.0\text{x}10^{-4}$	72
NPLI[1]	3	1 to 3	$3.0\text{x}10^{-6}$	$9.0\text{x}10^{-4}$	39
NIST3[2]	2	2 to 4	$3.0\text{x}10^{-6}$	$9.0\text{x}10^{-4}$	30
KRISS	3	4	$3.0\text{x}10^{-6}$	$9.0\text{x}10^{-4}$	72
NIST4	4	2	$3.0\text{x}10^{-6}$	$9.0\text{x}10^{-4}$	48

Notes:
1. NPLI calibration runs spanned multiple days.
2. NIST3 calibration runs spanned multiple days.

Table 5. Summary of voltages measured on ion gauge SI-404 at the beginning of the day for each calibration run at each cycle at each NMI. Listed are the filament bias voltages, grid bias voltages, and voltage drops across the 1 kΩ grid-line resistor.

NMI *j* Cycle *m*	Run	Date	Bias Voltages		Voltage Drop Grid-line resistor
			Filament	Grid	
NIST1	1	8/11/1998	29.87	179.9	4.018
	2	8/13/1998	29.85	179.8	4.014
	3	8/18/1998	29.84	179.8	4.014
	4	8/21/1998	29.84	179.8	4.014
	5	8/26/1998	29.84	179.8	4.014
	6	8/31/1998	29.84	179.8	4.014
	7	9/3/1998	29.84	179.8	4.014
PTB1	1	2/25/1999	29.83	180.0	4.011
	2	3/1/1999	29.83	180.0	4.012
	3	3/4/1999	29.83	180.0	4.013
NPL	1	4/20/1999	29.83	180.0	4.011
	2	4/22/1999	29.83	180.0	4.011
PTB2	1	6/9/1999	27.64	175.9	4.008
	2	6/14/1999	29.80	180.0	4.008
NIST2	1	1/6/2000	29.81	180.1	4.012
	2	1/10/2000	29.80	180.0	4.014
	3	1/13/2000	29.80	180.1	4.013
	4	1/21/2000	29.80	180.0	4.015
	5	1/27/2000	29.79	180.0	4.014
NPLI	1	6/26/2000	29.81	179.8	4.008
	1	6/27/2000	29.82	179.8	4.011
	2	6/28/2000	29.82	179.9	4.011
	3	7/10/2000	29.81	179.9	4.012
	3	7/11/2000	29.81	179.9	4.011
	3	7/12/2000	29.81	179.9	4.012
NIST3	1	2/6/2001	29.81	180.0	4.007
	1	2/8/2001	29.81	180.0	4.010
	2	2/13/2001	29.81	180.0	4.010
KRISS	1	11/14/2001	29.79	176.5	4.009
	2	11/16/2001	29.79	180.1	4.009
	3	11/21/2001	29.80	180.1	4.009
NIST4	1	4/23/2002	29.82	180.2	4.009
	2	4/25/2002	29.82	180.2	4.011
	3	4/29/2002	29.82	180.2	4.012
	4	5/2/2002	29.82	180.2	4.011

the ionization gauges, pressure-*dependent* shifts in the ionization gauge characteristics, pressure-*independent* shifts in the ionization gauge characteristics and the normalization of the ionization gauge response to the spinning rotor gauge response at the common pressure of 9×10^{-4} Pa, and long-term shifts in both the ionization gauge and spinning rotor gauge responses. As mentioned in Sec. 4.2, the Stabil-Ion gauge SI-404 was the only ionization gauge calibrated by all participants, so the comparison for pressures below 9×10^{-4} Pa is based solely on that gauge. Section 6.1 discusses zero-pressure offsets, which were applied to all the gauges. Other factors are discussed in context with the data analysis for the SRGs (Sec. 6.2) and the ion gauge (Sec. 6.5) as appropriate. The goal of the analysis is to determine a *calibration ratio* for each transfer standard, each NMI, and at each pressure; this represents the ratio of the indicated pressure of the transfer standards to the measured/generated pressure of the primary standard. This calibration ratio is then used to determine the indicated pressure achieved by the transfer standards, if the primary standards of the NMI were set to the exact same measured/generated pressure. This approach is used to account for slight differences between the measured/generated pressures and the nominal target pressures. A comparison of these indicated gauge pressures of the transfer standards at the NMIs is used to determine the degree of equivalence to a reference value and the degree of equivalence between NMIs.

The subscript nomenclature used is as follows: the "*i*" index refers to the transfer standard gauge; index "*j*" refers to the NMI making the measurement; index "*m*" refers to the calibration cycle for PTB and NIST; and index "*k*" is the individual reading of the gauge.

6.1 Corrections for zero pressure offset

The gauge readings are first corrected for their "zero" reading with the vacuum chamber evacuated and at the base pressure:

$$p_{ijmk} = p_{Gijmk} - p_{G0ijmk} \ . \tag{1}$$

Here, p_{Gijmk} is the uncorrected gauge reading, p_{G0ijmk} is the zero-pressure gauge reading, and p_{ijmk} is the gauge reading corrected for zero-pressure offsets. For series expansion standards, p_{G0ijmk} is measured just prior to every expansion; for orifice flow standards, it is measured before any gas flow is established. For both methods, the zero-pressure reading is assumed not to change during the course of the measurements.

6.2 Calibration ratio and pressure comparison at 9×10^{-4} Pa based on the spinning rotor gauges

The SRGs are nominally linear devices, and the ratio of the transfer standard pressure reading to the primary standard pressure will be independent of pressure, around the target pressure of 9×10^{-4} Pa. For SRG *i,* NMI *j*, cycle *m*, reading *k* (total of N_{ijm} readings), the average calibration ratio, a_{ijm}, (commonly referred to as accommodation coefficient for

SRGs)[10] is:

$$a_{ijm} = \frac{1}{N_{ijm}} \sum_{k=1}^{N_{ijm}} a_{ijmk} = \frac{1}{N_{ijm}} \sum_{k=1}^{N_{ijm}} \frac{p_{ijmk}}{P_{jmk}} \ . \tag{2}$$

i has the values 1 (for SRG-027) and 2 (for SRG-030); *jm* has values NIST1, NIST2, NIST3, NIST4 (for the 4 cycles at NIST), PTB1, PTB2 (2 cycles at PTB), NPL, NPLI, and KRISS. P_{jmk} is the measured/generated pressure of the NMI standard. The SRG pressure is:

$$p_{ijmk} = \sqrt{\frac{8RT_{jmk}}{\pi M}} \frac{\pi d_i \rho_i}{20} \left(DCR_{ijmk} - RD_{ijmk}(\omega) \right) \ . \tag{3}$$

Here, the zero-pressure reading is accounted for in the second term of the parenthesis, given by the "residual drag" or *RD*. T_{jmk} is the gas temperature of the standard, d_i and ρ_i are the diameter and density of the SRG rotor, *R* is the universal gas constant, and *M* is the molar mass of argon. The term *DCR* (deceleration rate) is given by:

$$DCR_{ijmk} = \left(\frac{\dot{\omega}}{\omega} \right)_{ijmk} \ . \tag{4}$$

The rotor rotational frequency is given by ω and the time rate of rotational decay of the rotor is given by $\dot{\omega}$. The number of repeat readings, N_{ijm}, is the total number of times the pressure level has been independently generated, which is the number of data points on each calibration run summed over the number of runs. N_{ijm} is listed in Table 3; except for cycle NIST1, $N_{1jm} = N_{2jm}$. At each generated pressure, most participants recorded the SRG readings multiple times and computed a short-term average and standard deviation. The assumption of the analysis is that run-to-run variability is dominant over within-run variability, *i.e.*, each realization of the generated pressure represents a different parent population for the subsequent SRG readings taken over a short time period after each pressure was realized.

Figure 1 presents the calibration ratios (a_{ijm}) for the two SRGs as determined by all the cycles of all the participants. The *x*-axis shows the chronological progression in the comparison. The calibration ratio for SRG-030 was higher than for SRG-027 for all NMIs. The maximum relative difference between NMIs was about 2.3 % for both SRG-027 and SRG-030. Figure 2 shows the shift in the calibration ratio for the four calibration cycles at NIST; each data set is normalized by the first NIST calibration ratio for each SRG, $a_{i\text{NIST1}}$. The relative standard deviation of the four NIST values was 0.41 % and 0.83 % for SRG-027 and SRG-030, respectively. The relative shift from PTB1 to PTB2 was −0.48 % for SRG-027 and 0.59 % for SRG-030.

[10] We use the symbol *a* instead of σ for the accommodation coefficient to avoid duplication with the use of σ for standard deviation. The calibration ratio a_{ijm} is the inverse of the gauge correction factor *CF* defined in the protocol.

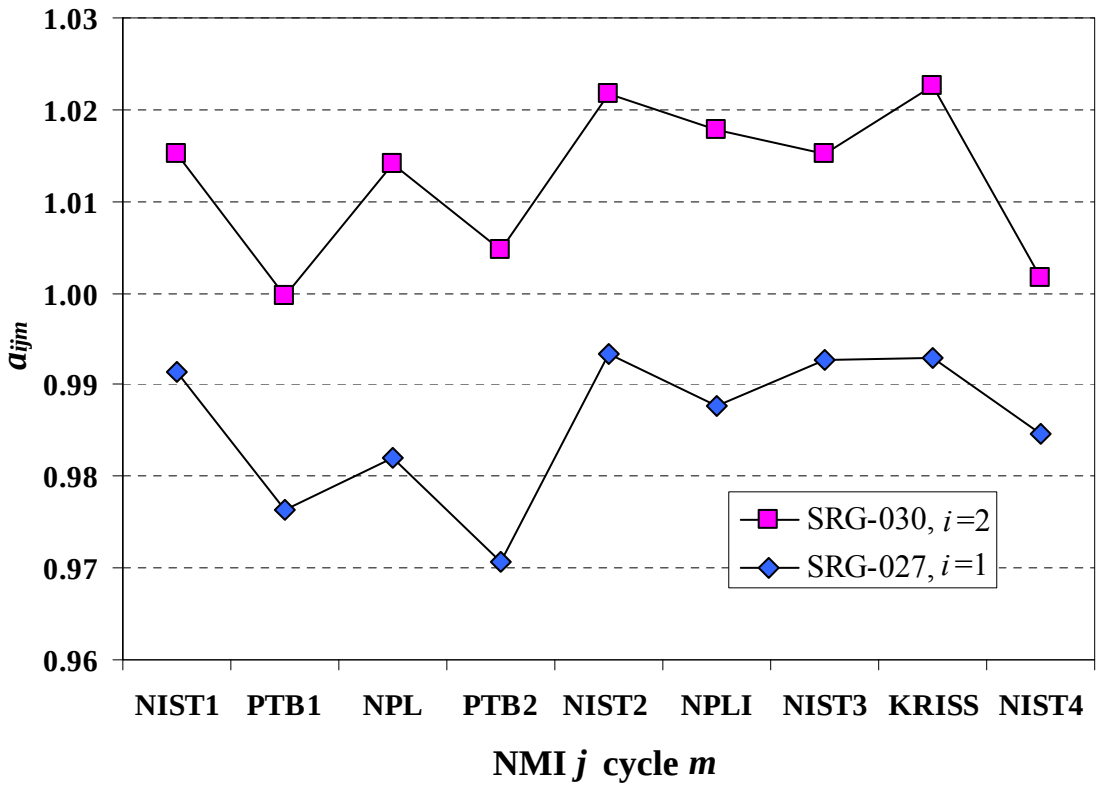

Figure 1. Calibration ratio a_{ijm} (accommodation coefficient) for SRG-027 and SRG-030 at each calibration cycle at the NMIs, 9×10^{-4} Pa. Data shown in chronological order.

The calibration ratio is used to calculate a *predicted gauge pressure reading* on SRG i when primary standard of NMI j (at calibration cycle m) is set to target pressure, P_T:

$$p_{ijm} = a_{ijm} P_T \quad . \tag{5}$$

The predicted gauge reading of eq. (5) (designated by the inclusion of subscripts j and m) is not the same as that of eq. (3); p_{ijmk} is the actual reading of the SRG during the calibration, whereas p_{ijm} is the predicted reading of the SRG when the primary standard is set to pressure P_T. The calibration ratios and predicted gauge pressure readings are presented in Sec. 7.1.

In order to compare the pressures of the NMIs to a reference pressure and to each other, a single gauge "pressure" is desired that includes the effects of both SRGs and the multiple calibration cycles. For each calibration cycle of each NMI, a *mean cycle gauge pressure reading* p_{jmU} was calculated as the simple arithmetic mean of the predicted gauge readings of the two SRGs:

$$p_{jmU} = \frac{p_{1jm} + p_{2jm}}{2} \quad , \tag{6}$$

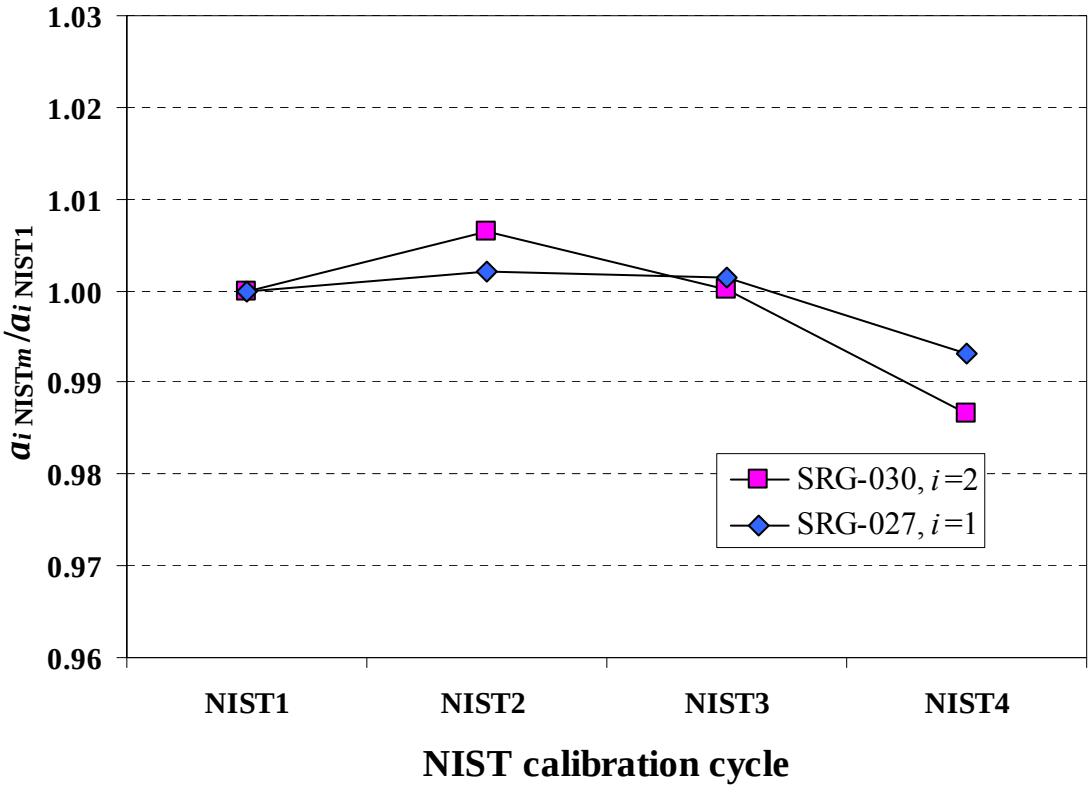

Figure 2. NIST calibration ratio ($a_{i\mathrm{NIST}m}$) normalized to NIST1 calibration ratio ($a_{i\mathrm{NIST1}}$), for SRG-027 and SRG-030, 9×10^{-4} Pa.

where the subscript *U* denotes that the gauge readings are uncorrected to the target pressure (explanation to follow), and *m* refers to the cycle of the NMI. The arithmetic mean was chosen instead of a weighted mean, because the variances of the predicted gauge readings are dominated by the variances due to long-term shifts of the SRGs, and these variances are based on limited measurements of the pilot laboratory and PTB (see Sec. 6.3). Use of the weighted mean requires well-known variances [12].

For NPL, NPLI, and KRISS, the subscript *m* can be dropped in eq. (6) to define p_{jU} as the *mean gauge pressure reading*, as these NMIs had only one calibration cycle. For the pilot laboratory (NIST), following the analysis of [13] and [14], a single value of p_{jU} was calculated as the arithmetic mean of the four cycles. For PTB, a single value of p_{jU} was calculated as the arithmetic mean of the two cycle values:

$$p_{jU} = \frac{1}{n_j}\sum_{m=1}^{n_j} p_{jmU} \;,\; n_j = 4 \text{ (NIST)},\; n_j = 2 \text{ (PTB)}. \qquad (7)$$

Implicit in use of the arithmetic mean for calculating p_{jU} for NIST and PTB is the assumption that changes in the calibration ratio of the SRGs are best approximated by a constant model. The changes in $a_{i\mathrm{NIST}m}$ from successive cycles (e.g., NIST1 to NIST2) are, in 5 out of 6 cases, larger than the Type A uncertainty of each cycle. This indicates there were actual changes in $a_{i\mathrm{NIST}m}$ between the NIST cycles, and therefore between cycles at NIST and the other NMIs. However, there is no obvious trend of decreasing or increasing $a_{i\mathrm{NIST}m}$ with successive NIST cycles: 2 times there was an increase, 3 times there was a decrease, and once there was no change. In addition, there is no clear correlation between changes in $a_{i\mathrm{NIST}m}$ at NIST for cycles 1 and 2, to changes in $a_{i\mathrm{PTB}m}$ at PTB for cycles 1 and 2; for SRG-027 the changes at PTB were opposite in sign and larger in magnitude than at NIST, while for SRG-030 the changes at PTB were of the same sign and of similar magnitude as at NIST. In an earlier key comparison utilizing SRGs [15], a linear drift model was used to estimate changes in a_i using the pilot laboratory calibrations. In that case there was a preponderance of evidence that the calibration ratio of two SRGs was decreasing with time. NIST experience with repeat calibrations on a large sample of SRGs indicates that both positive and negative changes in calibration ratios can occur [10]. Over several years, individual SRGs can exhibit upward drift, downward drift, or random change in accommodation coefficient [10].

As the constant model is simplest to implement and there is no compelling information that it is incorrect, that model is used here. The implication of using the constant model is that if an NMI and NIST could calibrate the SRGs simultaneously, the best estimate of a_i for NIST would be the arithmetic mean of the four cycles, rather than a mean of the adjacent NIST cycles.

The key comparison reference value (KCRV, or p_R) is determined using the participant results in the manner described in the appendix. In order to set the KCRV numerically equal to the target pressure, we correct the mean gauge pressure readings (p_{jU}) by a common scaling factor. The *corrected mean gauge pressure reading* can be expressed as:

$$p_j = f_C p_{jU} \quad . \tag{8}$$

The readings p_j were used to determine degrees of equivalence to the key comparison reference value and between the participants. The scaling factor f_C is determined together with the choice of the KCRV (see Appendix A).

It is important to note that f_C merely shifts all the mean gauge readings up or down, and it will have no influence on the agreement between participants or between participants and the KCRV. It may differ from a value of 1.0 if the transfer standard reads consistently low or high for all participants, or due to the distribution of gauge readings of the participants and the definition of the KCRV.

6.3 Estimates of uncertainty in the *predicted gauge pressure readings* at 9×10^{-4} Pa based on the SRGs

The combined standard uncertainty[11] in the predicted gauge pressure calculated using eq. (5), for each gauge i at each NMI j and each cycle m, is estimated from the root-sum-square of the component uncertainties [16]:

$$u_c(p_{ijm}) = \sqrt{u_B^2(p_{ijm}) + u_A^2(p_{ijm}) + u_{LTS}^2(p_{ijm})} \ , \tag{9}$$

where $u_B(p_{ijm})$ is the Type B standard uncertainty in p_{ijm} due to systematic effects in the primary standard of NMI j and systematic effects in SRG i; $u_A(p_{ijm})$ is the Type A standard uncertainty in p_{ijm} due to the combined short-term random errors of the SRGs and the primary standard j during calibration; and $u_{LTS}(p_{ijm})$ is the standard uncertainty arising from long-term shifts in the calibration ratio of the SRGs during the comparison.

The Type B standard uncertainty, derived from combining eqs. (2) and (3) into (5) is expressed as:

$$u_B(p_{ijm}) = \sqrt{u_{std}^2(p_{ijm}) + u_T^2(p_{ijm}) + u_{RD}^2(p_{ijm})} \ . \tag{10}$$

The component relative standard uncertainties are given by:

$$\frac{u_{std}(p_{ijm})}{p_{ijm}} = \frac{u_{std}(P_{jm})}{P_{jm}} \ , \tag{11}$$

$$\frac{u_T(p_{ijm})}{p_{ijm}} = \frac{u(T_{jm})}{2T_{jm}} \ , \tag{12}$$

$$\frac{u_{RD}(p_{ijm})}{p_{ijm}} = \frac{u(RD_{ijm})}{DCR_{ijm} - RD_{ijm}} \ . \tag{13}$$

Here, $u_{std}(P_{jm})$ is the standard uncertainty in the primary standards, $u(T_{jm})$ is the standard uncertainty in the gas temperature, and $u(RD_{ijm})$ is the standard uncertainty in the residual drag. P_{jm} is the arithmetic mean of the N_{ijm} readings of P_{jmk}; T_{jm} is the arithmetic mean of the N_{ijm} readings of T_{jmk}; $DCR_{ijm} - RD_{ijm}$ is a typical value for each SRG for cycle of each NMI.

Some parameters of eq. (3) (d, ρ, R, and M) are the same for all NMIs; because their values are completely correlated between NMIs, their uncertainty can be neglected in the determination of degrees of equivalence because they have no effect on comparisons of results between NMIs. There is no Type B uncertainty in the *DCR* measurement.

[11] All uncertainty terms designated by lower-case "*u*" letters are *standard* uncertainties, representing one standard deviation (coverage factor, k=1) of the quantity. All uncertainty terms designated by upper-case "*U*" letters are *expanded* uncertainties at the k=2 level.

Table 6 and Fig. 3 give the Type B relative standard uncertainty in pressure of the NMI primary standards, u_{std} at target pressure, P_T. For all cycles except PTB2, uncertainty values at $P_{jm} \approx P_T = 9.0\times10^{-4}$ Pa were used. For PTB2, the SRGs were calibrated at 3×10^{-3} Pa and 9×10^{-3} Pa so uncertainties at those pressures were used. The pressure of the primary standards is correlated between the two SRGs.

The standard uncertainty in the gas temperature, $u(T_{jm})$, was not requested in the protocol. Due to the correlation between temperature of the SRGs and the temperature used to determine the calculated/generated pressure, temperature errors will cancel out as long as both the SRG and the vacuum chamber have been corrected to the same temperature. However, if there are spatial variations in the chamber temperature, or if the chamber temperature is drifting in time and the SRG accommodation coefficient is not corrected (this could occur if the temperature entered in the SRG controller is not changed, or the accommodation coefficient is not corrected for temperature in the analysis of the SRG output) there will be an error. To avoid underestimating the uncertainty, we have used one-half the maximum gas temperature drift during a day as $u(T_{jm})$ for each cycle at each NMI. This component is the same for both SRGs, since it is assumed to arise from the same effect. It will be correlated between the two SRGs (hence the subscript i is dropped in the notation), and for all readings during the day (hence the subscript k is dropped as well). The results presented in Sec. 7.1 show that this component is small compared to other uncertainties, except for the Type A uncertainty.

The residual drag, *RD,* for the SRGs was not measured at the same time as *DCR*, but rather before or after the measurement. Hence there is a Type B standard uncertainty, $u(RD_{ijm})$, associated with whether *RD* at the time of the *DCR* measurement is the same as during its determination. Further, *RD* is generally a function of rotor frequency, ω, so the *RD* data should be fitted for frequency dependence and the measured ω during the *DCR* calibration used to compute *RD*. What follows is the method each NMI used for determining $u(RD_{ijm})$. For NIST, *RD* was measured before and after the *DCR* measurement on each day of each calibration cycle. The *RD* data was fit to a straight line vs. ω. The standard error of the fitted lines, for the multiple days making up a calibration cycle, were averaged to give $u(RD_{ijm})$ for that cycle. For PTB, *RD* was measured before the calibration cycle but not corrected for rotor frequency, because it was assumed by PTB that the normalization would occur at 9×10^{-3} Pa. At the higher pressure, this effect would have had a minor influence on the result. The uncertainty was estimated by assuming a rectangular distribution between the lowest and highest rotor frequency, and following [16], $u(RD_{ijm})$ was estimated as the half-width of the change in *RD* divided by $\sqrt{3}$. NPL used series expansion and determined *RD* immediately prior to expansion of the gas into the calibration chamber, that is, prior to each measurement of *DCR*. $u(RD_{ijm})$ was taken as the standard deviation about the mean *RD*. NPLI measured *RD* and its standard deviation before and after each calibration point. The change in *RD* was usually larger then the standard deviation of the before and after measurements. The uncertainty was estimated by assuming a rectangular distribution of *RD* between the before and after measurements, so $u(RD_{ijm})$ was estimated as the half-width divided by $\sqrt{3}$. KRISS also did not correct *RD* for ω, and did not provide an estimate for

Table 6. Relative standard uncertainties (Type B only) in pressure ($u_{std}(P_T)/P_T$) of the primary standards as reported by the NMI participants.

P_T / Pa	$u_{std}(P_T)/P_T$				
	NIST	PTB	NPL	NPLI	KRISS
9.0×10^{-7}			0.0076		
3.0×10^{-6}	0.0054	0.0020	0.0055	0.0086	0.0067
9.0×10^{-6}	0.0033	0.0020	0.0048	0.0078	0.0047
3.0×10^{-5}	0.0021	0.0020	0.0046	0.0075	0.0054
9.0×10^{-5}	0.0020	0.0020	0.0046	0.0082	0.0069
3.0×10^{-4}	0.0017	0.0010	0.0036	0.0083	0.0054
9.0×10^{-4}	0.0017	0.0010	0.0035	0.0076	0.0047
3.0×10^{-3}		0.0011	0.0035		
9.0×10^{-3}		0.0014			

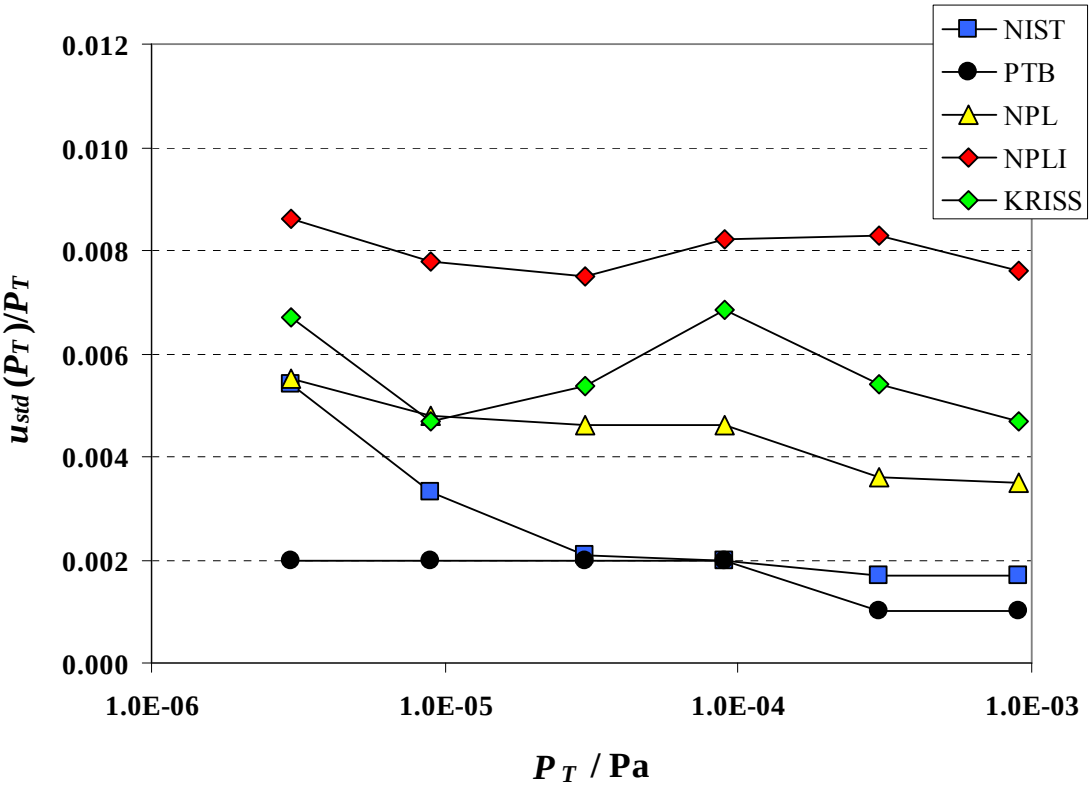

Figure 3. Relative standard uncertainties in pressure, $u_{std}(P_T)/P_T$, of the primary standards at the participating NMIs.

the uncertainty. Because they determined *RD* in a manner similar to PTB1, $u(RD_{ijm})$ of PTB1 was used for KRISS.

An additional Type B standard uncertainty is included for PTB2 only, which is added in quadrature with the other terms in eq. (10). For PTB2, the calibration ratios were measured at 3×10^{-3} Pa and 9×10^{-3} Pa, rather than at 9×10^{-4} Pa. An additional extrapolation standard uncertainty, u_{ext}, estimates the possible shift in calibration ratio from the values at the measured pressure to the values at the target pressure. u_{ext} is set at the difference between the measured values at 3×10^{-3} Pa and 9×10^{-3} Pa, assuming there could be a similar shift as pressure is decreased to 9×10^{-4} Pa. The relative standard uncertainties are 0.00003 for SRG-027 and 0.00046 for SRG-030.

The relative Type A standard uncertainty of each SRG in combination with the primary standard is given by the standard deviation of the mean, corrected for limited sample size [15, 17]:

$$\frac{u_A(p_{ijm})}{p_{ijm}} = \frac{u_A(a_{ijm})}{a_{ijm}} = \frac{s(a_{ijm})}{a_{ijm}} \sqrt{\frac{N_{ijm}-1}{N_{ijm}-3}} \quad , \tag{14}$$

where $s(a_{ijm})$ is the standard deviation of the mean of the repeat measurements a_{ijm}.

The standard uncertainty due to long-term shifts, $u_{LTS}(p_{ijm})$, is estimated using information on repeated calibrations of the transfer standards at NIST and PTB during the comparison. Prior to the comparison, NIST had no data on long-term performance of these two artifacts. Past international comparisons using vacuum gauge artifacts have also used repeated measurements at the pilot laboratory during the course of the comparison to characterize the uncertainty due to long-term shifts [11, 13, 14, 15]. One method [11, 15] assumes that the pilot laboratory value of a_i, at the time of the participant measurement of a_i, would be midway between the pilot laboratory value taken before and after the participant measurement. According to this method, an estimate of $u_{LTS}(a_i)$ is taken as one-half of the difference of the before and after values. This method assumes that shifts in a_i are more likely systematic than random (in shipping the artifacts from A to B to A, the change from A to B is the same in magnitude and direction as the change from B to A); the only information relevant to predicting the transport stability for each participant is the pilot laboratory values before and after the participant measurement. This method is appropriate if the artifacts are believed to be changing as a monotonic drift over time within a loop.

In [13] and [14], a constant model was used to characterize the changes in the artifact behavior, which is appropriate if the changes are believed to be random. As the statistical sample of the pilot laboratory in [13] and [14] was limited (three), a Type B evaluation was used to estimate u_{LTS} of each gauge. The variation due to long-term shifts was modeled as a normal distribution, with the standard uncertainty due to long-term shifts equal to one-half the difference between the maximum and minimum values of the pilot laboratory.

In the present work, as argued in Sec. 6.2, we also use a constant model to approximate the changes in the two SRG calibration ratios. This implies that the long-term shift in the calibration ratio is more random than systematic. The standard uncertainty due to those changes will be the same for all cycles of all participants. If the changes are indeed random, then the changes at PTB should have the same level of random variability as the changes at NIST. Hence we use all six instances where the calibration ratio was measured repeatedly at an NMI: the four changes in the NIST calibration ratios from the NIST mean, plus the two changes in the PTB calibration ratios from the PTB mean. We first calculate a pooled relative standard deviation of the six calibration ratio changes, $\sigma_{LTS}(a_i)$:

$$\frac{\sigma_{LTS}(a_i)}{a_i} = \frac{1}{\sqrt{n_r - 2}} \sqrt{\frac{\sum_{m=1}^{4} (a_{i\mathrm{NIST}m} - \langle a_{i\mathrm{NIST}} \rangle)^2}{\langle a_{i\mathrm{NIST}} \rangle^2} + \frac{\sum_{m=1}^{2} (a_{i\mathrm{PTB}m} - \langle a_{i\mathrm{PTB}} \rangle)^2}{\langle a_{i\mathrm{PTB}} \rangle^2}} \quad . \tag{15}$$

Here, $\langle a_{i\mathrm{NIST}} \rangle$ is the arithmetic mean of the four $a_{i\mathrm{NIST}m}$ calibration ratios, $\langle a_{i\mathrm{PTB}} \rangle$ is the arithmetic mean of the two $a_{i\mathrm{PTB}m}$ calibration ratios, and $n_r = 6$. This is further modified by applying the Bayesian correction for limited sample size [15, 17]; because two degrees of freedom are lost due to the pooling of the data, the appropriate effective sample size for the Bayesian correction is $n_b = 5$. The relative standard uncertainty due to long-term shifts is:

$$\begin{aligned} \frac{u_{LTS}(p_{ijm})}{p_{ijm}} = \frac{u_{LTS}(a_{ijm})}{a_{ijm}} &= \sqrt{\frac{n_b - 1}{n_b - 3}} \cdot \frac{\sigma_{LTS}(a_i)}{a_i} \\ &= \sqrt{\frac{4}{2 \cdot 4}} \cdot \sqrt{\frac{\sum_{m=1}^{4} (a_{i\mathrm{NIST}m} - \langle a_{i\mathrm{NIST}} \rangle)^2}{\langle a_{i\mathrm{NIST}} \rangle^2} + \frac{\sum_{m=1}^{2} (a_{i\mathrm{PTB}m} - \langle a_{i\mathrm{PTB}} \rangle)^2}{\langle a_{i\mathrm{PTB}} \rangle^2}} \end{aligned} \tag{16}$$

Values for the two SRGs are given in Table 7 in the row for $P_T = 9 \times 10^{-4}$ Pa.

In summary, the combined standard uncertainty in the predicted gauge pressure reading ($u_c(p_{ijm})$) is found from substitution of the Type B components of eqs. (11), (12), and (13) into eq. (10); the combined Type B components, Type A component (eq. (14)), and long-term stability component (eq. (16)) are then substituted into eq. (9).

6.4 Estimates of uncertainty in the *mean gauge pressure readings* and *corrected mean gauge pressure readings* at 9×10^{-4} Pa based on the SRGs

The standard uncertainty in the mean gauge pressure readings, $u_c(p_{jU})$, is found by applying the methods of [16] to eqs. (6) and (7). Recall that the measured/generated pressure of the primary standard is correlated for both SRGs and for multiple cycles at NIST and PTB. The gas temperature is correlated for both SRGs but not for the multiple cycles. In the equations that follow, the *i* subscript is dropped for components correlated between SRGs, and the *m*

Table 7. Summary of 1) relative standard uncertainty due to long-term shifts (u_{LTS}) in SRG-027, SRG-030, and SI-404; and 2) relative standard deviation of ion gauge inverse correction factor (S_{NIST}) and SRG calibration ratio (a_{NIST}) from 4 NIST calibration cycles. u_{LTS} is determined from standard deviation of 4 NIST calibration cycles and 2 PTB calibration cycles of either a_{ijm} (SRGs) or $\hat{S}_{jm}$ (ion gauge).

P_T / Pa	Gauge	u_{LTS}/p_{ijm} or u_{LTS}/p_{jm}	$\sigma(S_{\mathrm{NIST}})/S_{\mathrm{NIST}}$ or $\sigma(a_{i\,\mathrm{NIST}})/a_{i\,\mathrm{NIST}}$
3×10^{-6}	SI-404	0.01876	0.00648
9×10^{-6}	SI-404	0.01274	0.00670
3×10^{-5}	SI-404	0.01098	0.00857
9×10^{-5}	SI-404	0.00553	0.01185
3×10^{-4}	SI-404	0.00260	0.01441
9×10^{-4}	SI-404	0.00000	0.01593
	SRG-027	0.00577	0.00406
	SRG-030	0.01047	0.00830

subscript is dropped for components correlated between cycles. For the three NMIs that measured the SRGs for one cycle, the combined standard uncertainty was estimated as:

$$u_c(p_{jU}) = \left(u_{std}^2(p_j) + u_T^2(p_j) + \frac{1}{4}\sum_{i=1}^{2}\left(u_{RD}^2(p_{ij}) + u_A^2(p_{ij}) + u_{LTS}^2(p_{ij}) \right) \right)^{1/2} . \qquad (17)$$

For the pilot laboratory (NIST), p_{jU} is the mean of 8 values of p_{ijm} (2 gauges, 4 cycles):

$$u_c(p_{jU}) = \left(u_{std}^2(p_j) + \frac{1}{16}\sum_{m=1}^{4} u_T^2(p_{jm}) + \frac{1}{64}\sum_{m=1}^{4}\sum_{i=1}^{2}\left(u_{RD}^2(p_{ijm}) + u_A^2(p_{ijm}) + u_{LTS}^2(p_{ijm}) \right) \right)^{1/2} \qquad (18)$$

For PTB, p_{jU} is the mean of 4 values of p_{ijm}, or

$$u_c(p_{jU}) = \left(\begin{array}{l} \left(\sum_{m=1}^{2} \frac{u_{std}(p_{jm})}{2} \right)^2 + \frac{1}{4}\sum_{m=1}^{2} u_T^2(p_{jm}) + \\ + \frac{1}{16}\sum_{m=1}^{2}\sum_{i=1}^{2}\left(u_{RD}^2(p_{ijm}) + u_{ext}^2(p_{ijm}) + u_A^2(p_{ijm}) + u_{LTS}^2(p_{ijm}) \right) \end{array} \right)^{1/2} . \qquad (19)$$

The uncertainty of the primary standard is averaged for PTB because it has different magnitudes for cycle 1 and cycle 2, but they arise from the same correlated source. The uncertainty due to extrapolation, u_{ext}, is included for PTB2 only. Note that the multiple calibration cycles for NIST and PTB tend to reduce the uncertainties from uncorrelated quantities arising from the short-term and long-term variability of the SRGs. Values for uncertainty components will be listed in Sec. 7.1. Values for uncertainties in the corrected mean gauge pressure reading, $u_c(p_j)$, are found from evaluating the uncertainty of eq. (8):

$$u_c(p_j) = f_C u_c(p_{jU}) \ . \tag{20}$$

6.5 Calibration ratio and pressure comparison from 3×10^{-6} Pa to 3×10^{-4} Pa based on the ionization gauge

Comparisons for the pressure range (3×10^{-6} to 3×10^{-4} Pa) are based on measurements of ionization gauge SI-404. In the equations that follow, the *i* subscript (which refers to the transfer standard gauge) is dropped since it has only one value. The target pressures, P_T, for the comparisons were 3×10^{-6} Pa, 9×10^{-6} Pa, 3×10^{-5} Pa, 9×10^{-5} Pa, 3×10^{-4} Pa, and 9×10^{-4} Pa. Measurements at 9×10^{-4} Pa were used to correct for pressure-independent shifts in the ion gauge characteristics, as described below. For each NMI *j* and each calibration cycle *m*, an average ion gauge inverse correction factor[12], $S_{jm}(P_{jm})$, was calculated from the N_{jm} readings of the measured/generated pressure P_{jmk}:

$$S_{jm}(P_{jm}) = \frac{1}{N_{jm}} \sum_{k=1}^{N_{jm}} S_{jmk}(P_{jmk}) = \frac{1}{N_{jm}} \sum_{k=1}^{N_{jm}} \frac{p_{jmk}}{P_{jmk}} \ . \tag{21}$$

In eq. (21), the ion gauge pressure readings, p_{jmk}, have been adjusted for zero-pressure offsets as in eq. (1). Since the primary standards operated at different temperatures and the ionization gauges are sensitive to gas density ([11] and [18]), equivalent inverse correction factors were determined for the common reference temperature of 23 ºC. This was done by multiplying the individual inverse correction factors (prior to averaging of eq. (21)) by the ratio of the absolute temperature of the standard divided by 296.15 K.

P_{jm} is the arithmetic mean of the N_{jm} measured/generated pressures on the NMI standard. The average ion gauge inverse correction factors were then corrected to values at the target pressures, since the measured pressures (both P_{jmk} and the mean P_{jm}) of the NMI standards usually differed from the target pressure. Results presented in Sec. 7.2 show that the inverse correction factors varied with pressure. This *pressure-dependent* correction was done by assuming a linear variation in S_{jm} from the value at P_{jm} to the value at the target pressure P_T. Values of S_{jm} bounding the pressure interval are used in the linear interpolation. The uncertainty introduced by this correction is assumed to be negligible, as the deviations from the target pressures are small, and the magnitude of the correction ranges from 5 times

[12] S_{jm} is the inverse of the correction factor CF defined in the protocol.

smaller to 75 times smaller than the standard uncertainty of the ion gauge inverse correction factor. The result is a set of $S_{jm}(P_T)$ values.

Next a *pressure-independent* correction is applied to the entire set of data at each NMI for each calibration cycle [11]. This normalization comes from assuming the generated pressure of the primary standard of the NMI, at 9×10^{-4} Pa, was the same whether it was being measured with an ion gauge or an SRG. The ion gauge *calibration ratio*, $K_{jm}(P_T)$, is defined such that the predicted gauge pressure reading using the ion gauge is the same as the mean gauge pressure reading from the SRGs at 9×10^{-4} Pa :

$$K_{jm}(P_T) = \frac{S_{jm}(P_T)}{S_{jm}(9\times10^{-4})} \cdot \frac{\hat{p}_{jU}}{\hat{p}_R} = \hat{S}_{jm}(P_T) \cdot \frac{\hat{p}_{jU}}{\hat{p}_R}$$

with: (22)

$$\hat{S}_{jm}(P_T) = \frac{S_{jm}(P_T)}{S_{jm}(9\times10^{-4})}$$

$\hat{p}_{jU}$ is the value of p_{jU} determined from the SRGs at 9×10^{-4} Pa, and $\hat{p}_R$ is numerically equal to 9×10^{-4} Pa and is determined from the SRG data. The parameter $\hat{S}_{jm}(P_T)$ is a normalized ion gauge inverse correction factor, taking on the value 1.0 (by definition) at 9×10^{-4} Pa. For the NMIs with multiple calibration cycles, we are assuming that the vacuum standards perform identically over time, and $\hat{p}_{jU}$ is representative of the behavior of the standard at 9×10^{-4} Pa for all cycles. Note that p_{ijm} changes between cycles due to shifts in the SRGs, and is therefore not used in the normalization. Experimental results presented in Sec. 7.2 will show the smaller variability in a_{ijm} compared to the variability in $S_{jm}(9\times10^{-4})$, which supports using the SRG results to normalize the ion gauge readings.

The remaining analysis for the ion gauge follows closely to that of the SRGs. The calibration ratio may be used to calculate a *predicted gauge pressure reading* when primary standard of NMI *j* (at calibration cycle *m*) is set to target pressure, P_T:

$$p_{jm} = K_{jm}(P_T) \cdot P_T \ . \tag{23}$$

The calibration ratios and predicted gauge pressure readings are presented in Sec. 7.2. For NPL, NPLI, and KRISS, the subscript *m* can be dropped in eq. (23), giving p_{jU} that is referred to as the *mean gauge pressure reading*[13]. For NIST and PTB, a single value of p_{jU} was calculated as the arithmetic mean of the multiple cycles:

$$p_{jU} = \frac{1}{n_j}\sum_{m=1}^{n_j} p_{jm} \ , \ n_j = 4 \text{ (NIST)}, \ n_j = 2 \text{ (PTB)}. \tag{24}$$

[13] Although there is no averaging occurring for NPL, NPLI, and KRISS in p_{jU}, we refer to the term as the mean gauge pressure reading for consistency with its definition for the SRGs.

As with the SRGs, the subscript *U* denotes that the gauge readings are uncorrected to the target pressure. The results of Sec. 7.2 show that changes in K_{jm} for NIST appear to be random with both positive and negative shifts between cycles, which is consistent with using a constant model to approximate the changing quantity.

The *corrected mean gauge pressure reading* is defined such that when the KCRV is determined from participant pressures, it will numerically equal the target pressure. The scaling factor $f_C(P_T)$ is applied to all participants:

$$p_j = f_C(P_T) \cdot p_{jU} \ . \tag{25}$$

As with the comparison at 9×10^{-4} Pa based on the SRGs, the application of the common scaling factor has no effect on the participant-to-participant or participant-to-KCRV degrees of equivalence.

6.6 Estimates of uncertainty in the *predicted gauge pressure readings* from 3×10^{-6} Pa to 3×10^{-4} Pa based on the ionization gauge

The uncertainty analysis for the predicted gauge readings (p_{jm}) based on the ion gauges follows the method for the uncertainty based on the SRGs. However, we must also include the uncertainty due to the pressure-independent correction of eq. (22). The combined standard uncertainty, at each NMI *j* and each cycle *m*, in the predicted gauge pressure using the ion gauge, is [16]:

$$u_c(p_{jm}) = \sqrt{u_B^2(p_{jm}) + u_A^2(p_{jm}) + u_{LTS}^2(p_{jm})} \ . \tag{26}$$

The uncertainty terms are evaluated by using the definitions of p_{jm} and K_{jm} of eqs. (23) and (22), and expressing each term as a relative standard uncertainty. The long-term shift component, u_{LTS}, includes only the effects of the ionization gauge, whereas long-term shift effects due to the SRGs (resulting from the normalization of eq. (22)) are grouped with the Type B components. The Type B components, $u_B(p_{jm})$, are given by:

$$\frac{u_B(p_{jm})}{p_{jm}} = \sqrt{\left(\frac{u_{std}(P_T)}{P_T}\right)^2 + \left(\frac{u_{SRG}(\hat{p}_{jU})}{\hat{p}_{jU}}\right)^2} \ . \tag{27}$$

As in Sec. 6.3, u_{std} is the standard uncertainty in measured/generated pressure of the primary standard. The term $u_{SRG}(\hat{p}_{jU})$ is the standard uncertainty in the mean gauge pressure from the SRGs at 9×10^{-4} Pa, due to all short-term and long-term effects of the SRGs in eq. (17), (18), or (19). It does not include the uncertainty of the primary standard, since that quantity is perfectly correlated and cancels out by equating p_{jm} to $\hat{p}_{jU}$ at the common pressure:

$$u_{SRG}(\hat{p}_{jU}) = \sqrt{u_c^2(\hat{p}_{jU}) - u_{std}^2(\hat{p}_{jU})}\,. \tag{28}$$

For the NMIs with multiple calibration cycles (NIST and PTB), both quantities that are accounted for by the Type B terms in eq. (27) are correlated between cycles (and are identical), so the uncertainty they contribute will not be reduced by averaging.

The Type A standard uncertainties, $u_A(p_{jm})$, result from the combined short-term random errors of the ion gauge and the primary standard, evaluated both at P_T and at 9×10^{-4} Pa. The Type A standard uncertainty at 9×10^{-4} Pa must be included for all pressures due to the pressure-independent correction:

$$\frac{u_A(p_{jm})}{p_{jm}} = \sqrt{\left(\frac{u_A(S_{jm}(P_T))}{S_{jm}(P_T)}\right)^2 + \left(\frac{u_A(S_{jm}(9\times10^{-4}))}{S_{jm}(9\times10^{-4})}\right)^2}\,. \tag{29}$$

These components are calculated in the same manner as for the SRGs, using the standard deviation of the mean corrected for limited sample size [15, 17]:

$$\frac{u_A(S_{jm}(P_T))}{S_{jm}(P_T)} = \frac{s(S_{jm}(P_T))}{S_{jm}(P_T)}\sqrt{\frac{N_{jm}-1}{N_{jm}-3}}\,, \tag{30}$$

where $s(S_{jm}(P_T))$ is the standard deviation of the mean of the repeat measurements of $S_{jm}(P_T)$.

$u_{LTS}(p_{jm})$ is the standard uncertainty arising from long-term shifts in the normalized ion gauge inverse correction factor, $\hat{S}_{jm}(P_T)$. As with the SRG calibration ratios, we use a constant model to approximate the changes in $\hat{S}_{jm}(P_T)$ arising from the long-term shifts. This implies that the long-term shifts are more random than systematic. The relative uncertainty due to long-term shifts is assumed to be the same for all cycles at all NMIs. It is evaluated by the pooled relative standard deviation of $\hat{S}_{jm}(P_T)$ of the four NIST calibrations combined with the two PTB calibrations, applying the Bayesian correction for limited sample size ($n_r = 6$, $n_b = 5$):

$$\frac{u_{LTS}(p_{jm})}{p_{jm}} = \frac{u_{LTS}(\hat{S}_{jm}(P_T))}{\hat{S}_{jm}(P_T)} =$$
$$= \sqrt{\frac{n_b-1}{n_b-3}}\,\frac{1}{\sqrt{n_r-2}}\sqrt{\frac{\sum_{m=1}^{4}\left(\hat{S}_{\mathrm{NIST}m}(P_T) - \left\langle \hat{S}_{\mathrm{NIST}}(P_T)\right\rangle\right)^2}{\left\langle \hat{S}_{\mathrm{NIST}}(P_T)\right\rangle^2} + \frac{\sum_{m=1}^{2}\left(\hat{S}_{\mathrm{PTB}m}(P_T) - \left\langle \hat{S}_{\mathrm{PTB}}(P_T)\right\rangle\right)^2}{\left\langle \hat{S}_{\mathrm{PTB}}(P_T)\right\rangle^2}}\,. \tag{31}$$

The normalized form of the ion gauge inverse correction factor is used, because the uncertainties arising from long-term shifts at 9×10^{-4} Pa are accounted for in $u_{SRG}(\hat{p}_{jU})$. $\left\langle \hat{S}_{\mathrm{NIST}}(P_T) \right\rangle$ is the arithmetic mean of the four $\hat{S}_{\mathrm{NIST}m}(P_T)$ values, and $\left\langle \hat{S}_{\mathrm{PTB}}(P_T) \right\rangle$ is the arithmetic mean of the two $\hat{S}_{\mathrm{PTB}m}(P_T)$ values. Values for u_{LTS} are listed in Table 7.

In summary, the combined standard uncertainty in the predicted gauge pressure reading ($u_c(p_{jm})$) is found by substituting the Type B components of eqs. (27) and (28), the Type A component of eq. (29), and long-term stability component of eq. (31) into eq. (26).

6.7 Estimates of uncertainty in the *mean gauge pressure readings* and the *corrected mean gauge pressure readings* from 3×10^{-6} Pa to 3×10^{-4} Pa based on the ionization gauge

For the three NMIs that measured the ion gauge for one cycle, $p_{jU} = p_{jm}$, so the combined standard uncertainty $u_c(p_{jU})$ follows directly from eq. (26), or:

$$u_c(p_{jU}) = \left(u_B^2(p_{jm}) + u_A^2(p_{jm}) + u_{LTS}^2(p_{jm}) \right)^{1/2} . \tag{32}$$

For NIST and PTB, the component uncertainties in $u_c(p_{jm})$ will propagate to the combined standard uncertainty in the mean gauge reading $u_c(p_{jU})$ through eq. (24). The Type B uncertainties arise from components that are correlated between cycles, but the Type A and long-term shift uncertainties are due to quantities that are not correlated between multiple cycles. For NIST, p_{jU} is the mean of 4 values of p_{jm}, so:

$$u_c(p_{jU}) = \left(u_B^2(p_{jm}) + \frac{1}{16}\sum_{m=1}^{4} \left(u_A^2(p_{jm}) + u_{LTS}^2(p_{jm}) \right) \right)^{1/2} . \tag{33}$$

For PTB, p_{jU} is the mean of 2 values of p_{jmU}, or:

$$u_c(p_{jU}) = \left(u_B^2(p_{jm}) + \frac{1}{4}\sum_{m=1}^{2} \left(u_A^2(p_{jm}) + u_{LTS}^2(p_{jm}) \right) \right)^{1/2} . \tag{34}$$

Note that the multiple calibration cycles for NIST and PTB tend to reduce the uncertainties from uncorrelated quantities arising from the short-term and long-term variability of the ion gauge. The uncertainty in the corrected mean gauge pressure reading is given in eq. (20). Values for uncertainty components will be listed in the Sec. 7.2.

7. Results for the comparison

7.1 Results at 9×10^{-4} Pa using the two SRGs

The calibration ratios for the two SRGs at 9×10^{-4} Pa for each calibration cycle at each NMI are listed in Tables 8a and 8b. The tables also list the predicted gauge readings

Table 8a. Results for SRG-027 (i = 1) for each cycle at each NMI for 9×10^{-4} Pa. Listed are calibration ratio (a_{ijm}), predicted gauge reading (p_{ijm}), relative standard uncertainty contributions to $u_c(p_{ijm})$, and the combined standard uncertainty $u_c(p_{ijm})$.

NMI j Cycle m	SRG-027, i = 1								
	a_{1jm}	p_{1jm} / Pa	Relative standard uncertainties on p_{ijm}						$u_c(p_{1jm})$ / Pa
			u_A	u_{std}	u_{RD}	u_T	u_{LTS}	u_c	
NIST1	0.9913	8.922E-04	0.00021	0.00170	0.00043	0.00005	0.00577	0.00604	5.39E-06
PTB1	0.9764	8.787E-04	0.00116	0.00100	0.00330	0.00017	0.00577	0.00682	6.00E-06
NPL	0.9820	8.838E-04	0.00015	0.00350	0.00084	0.00008	0.00577	0.00681	6.01E-06
PTB2[1]	0.9707	8.736E-04	0.00016	0.00125	0.00392	0.00017	0.00577	0.00709	6.20E-06
NIST2	0.9933	8.940E-04	0.00032	0.00170	0.00069	0.00003	0.00577	0.00607	5.42E-06
NPLI	0.9876	8.888E-04	0.00032	0.00760	0.00113	0.00046	0.00577	0.00963	8.56E-06
NIST3	0.9927	8.934E-04	0.00189	0.00170	0.00047	0.00001	0.00577	0.00633	5.65E-06
KRISS	0.9930	8.937E-04	0.00183	0.00469	0.00330	0.00009	0.00577	0.00834	7.45E-06
NIST4	0.9846	8.861E-04	0.00078	0.00170	0.00034	0.00005	0.00577	0.00608	5.39E-06

Notes:
1. PTB2 data taken at 2.8×10^{-3} Pa and 8.2×10^{-3} Pa instead of 9.0×10^{-4} Pa. u_{std} is average of values at those pressures. u_c includes relative uncertainty of extrapolation of 0.00003.

Table 8b. Results for SRG-030 (i = 2) for each cycle at each NMI for 9×10^{-4} Pa. Listed are calibration ratio (a_{ijm}), predicted gauge reading (p_{ijm}), relative standard uncertainty contributions to $u_c(p_{ijm})$, and the combined standard uncertainty $u_c(p_{ijm})$.

NMI j Cycle m	SRG-030, i = 2								
	a_{2jm}	p_{2jm} / Pa	Relative standard uncertainties on p_{ijm}						$u_c(p_{2jm})$ / Pa
			u_A	u_{std}	u_{RD}	u_T	u_{LTS}	u_c	
NIST1	1.0151	9.136E-04	0.00018	0.00170	0.00058	0.00005	0.01047	0.01062	9.70E-06
PTB1	0.9996	8.997E-04	0.00090	0.00100	0.00165	0.00017	0.01047	0.01068	9.61E-06
NPL	1.0140	9.126E-04	0.00016	0.00350	0.00089	0.00008	0.01047	0.01107	1.01E-05
PTB2[1]	1.0046	9.041E-04	0.00030	0.00125	0.00205	0.00017	0.01047	0.01075	9.72E-06
NIST2	1.0216	9.195E-04	0.00020	0.00170	0.00056	0.00003	0.01047	0.01062	9.77E-06
NPLI	1.0179	9.161E-04	0.00049	0.00760	0.00068	0.00046	0.01047	0.01297	1.19E-05
NIST3	1.0152	9.137E-04	0.00211	0.00170	0.00042	0.00001	0.01047	0.01082	9.89E-06
KRISS	1.0226	9.203E-04	0.00090	0.00469	0.00165	0.00009	0.01047	0.01162	1.07E-05
NIST4	1.0016	9.015E-04	0.00061	0.00170	0.00084	0.00005	0.01047	0.01065	9.60E-06

Notes:
1. PTB2 data taken at 2.8×10^{-3} Pa and 8.2×10^{-3} Pa instead of 9.0×10^{-4} Pa. u_{std} is average of values at those pressures. u_c includes relative uncertainty of extrapolation of 0.00046.

Table 9. Summary of results at 9×10^{-4} Pa target pressure based on calibrations of the SRGs. Listed are mean gauge pressure reading (p_{jU}), uncertainty in mean gauge pressure reading $u(p_{jU})$, and its relative uncertainty $u(p_{jU})/p_{jU}$.

P_T / Pa	NMI j	p_{jU} / Pa	$u(p_{jU})$ / Pa	$u(p_{jU})$ / p_{jU}
$9\text{x}10^{-4}$	NIST	9.017E-04	3.12E-06	0.00346
	PTB	8.890E-04	4.11E-06	0.00462
	NPL	8.982E-04	6.25E-06	0.00695
	NPLI	9.024E-04	8.76E-06	0.00971
	KRISS	9.070E-04	7.15E-06	0.00788

(p_{ijm}) at a common target pressure of 9×10^{-4} Pa, and the components of standard uncertainty contributing to the combined standard uncertainty ($u_c(p_{ijm})$). The mean gauge reading (p_{jU}) and its uncertainty ($u_c(p_{jU})$), found from combining the results of the two gauges and multiple cycles, are listed in Table 9.

The calibration ratios for the two SRGs for the calibration cycles at each NMI were previously shown in Fig. 1. Figure 4 is a Youden plot of the predicted gauge pressure readings, p_{ijm}, and their standard uncertainties, $u_c(p_{ijm})$), plotted as the difference p_{1jm}-P_T on the x-axis and the difference p_{2jm}-P_T on the y-axis. The standard uncertainties are shown as the x and y error bars. p_{1jm} is the predicted gauge reading from SRG-027, and p_{2jm} is the predicted gauge reading from SRG-030. The Youden graphical representation has several important features. In the limit of large number of standards, random errors of precision in the primary standards are shown by a circular pattern of the data points. A relative bias between individual primary standards is revealed by a distribution along a diagonal, 45° to the positive x- and y-axis. Scatter of data perpendicular to this diagonal, particular for multiple cycles at the same NMI, provide a measure of precision (and long-term shifts) of the transfer standard gauges. As can be seen by Fig. 4, the PTB data appear to have a bias toward lower indicated pressure for both SRGs.

The largest component of the standard uncertainty for the predicted gauge pressure based on SRG-030 is u_{LTS}. For SRG-027, u_{LTS} is the largest component for all NMIs except NPLI. For NPLI, u_{std} is the largest component. For KRISS, u_{std} is slightly smaller than u_{LTS}; for PTB1 and PTB2, u_{RD} is slightly smaller than u_{LTS}; and for NPL, u_{std} is slightly smaller than u_{LTS}. The combined relative standard uncertainties range from 0.60 % to 0.96 % based on SRG-027, and they range from 1.06 % to 1.30 % based on SRG-030.

The mean gauge pressure reading for each NMI, p_{jU}, is plotted in Fig. 5 with the expanded (k=2) uncertainty shown as an error bar. As can be seen, the uncertainty bars overlap the target pressure 9×10^{-4} Pa for all NMIs except PTB. Recall that the KCRV is not yet defined, there is no scaling factor in p_{jU}, and lack of overlap with the target pressure does not

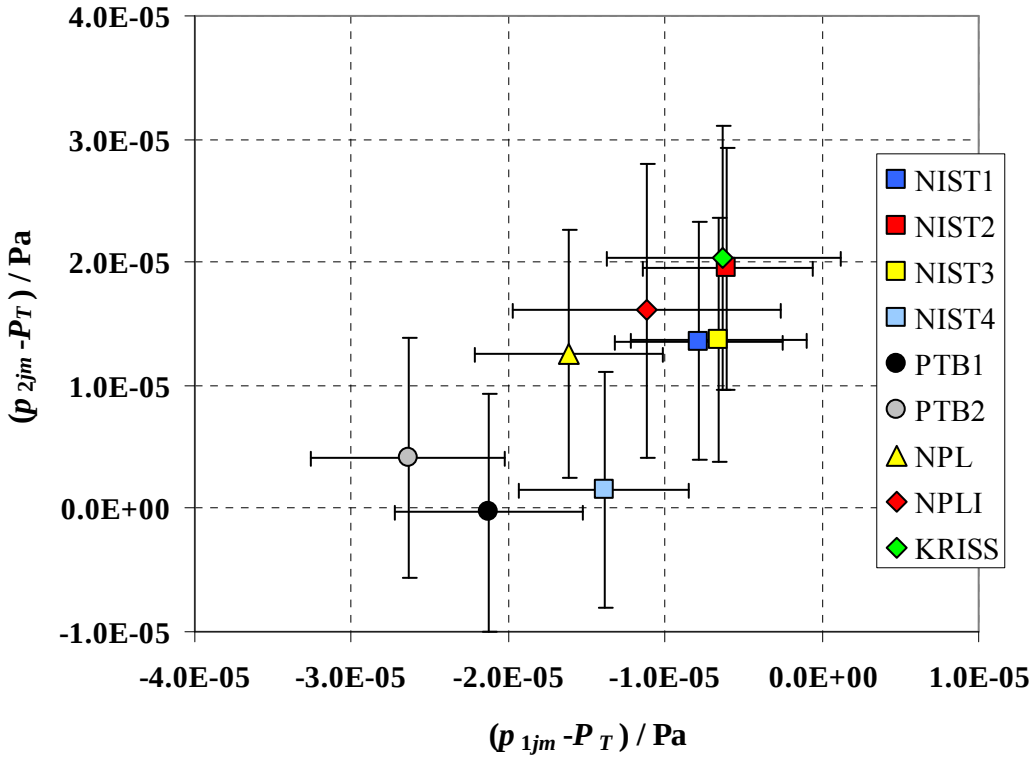

Figure 4. Youden plot of differences (p_{ijm}-P_T) between predicted gauge pressure readings of SRGs and measured/generated pressure of primary standards, when equal to a target pressure of 9×10^{-4} Pa. Error bars are combined standard uncertainty in the predicted gauge reading. SRG-027 (i=1) shown on x-axis and SRG-030 (i=2) shown on y-axis.

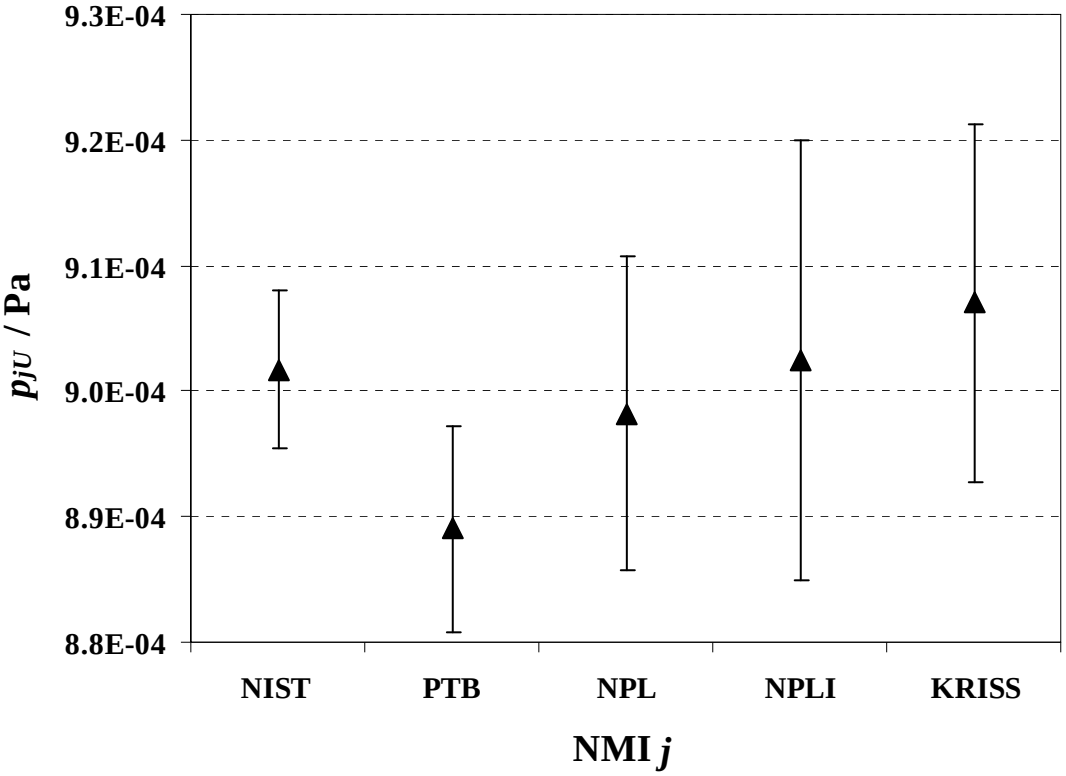

Figure 5. Mean gauge pressure reading (p_{jU}), with primary standards set at 9×10^{-4} Pa, for each NMI. Expanded (k=2) uncertainty in mean gauge reading shown as error bars.

necessarily imply lack of equivalence. The relative standard uncertainty in the mean gauge readings range from 0.35 % to 0.97 %.

7.2 Results from 3×10^{-6} Pa to 3×10^{-4} Pa based on the ionization gauge

The results for the measurements using ion gauge SI-404 for each calibration cycle at each NMI are listed in Table 10. This table lists the ion gauge inverse correction factor, S_{jm}, corrected to the reference temperature and target pressure; its Type A relative standard uncertainty, $u_A(S_{jm})/S_{jm}$; the calibration ratio, K_{jm}; the predicted gauge reading, p_{jm}; the component standard uncertainties contributing to the uncertainty in p_{jm}; and the combined standard uncertainty, $u_c(p_{jm})$. Results for PTB and NPL are also listed for target pressures outside the required range. The ion gauge inverse correction factors are plotted for all calibration cycles in Fig. 6. There is a general trend of increasing S_{jm} as pressure increases. At each pressure, the maximum variation between NMIs was about 4 %. The NIST results are separated out in Figs. 7a and 7b. Figure 7a plots S_{jm}, which shows shifts between the four calibrations at all pressures. The maximum variation occurred at 9×10^{-4} Pa, and was 3.5 %.

The relative standard deviation of S_{NIST} is listed in Table 7, which ranged from 0.65 % at 3×10^{-6} Pa to 1.6 % at 9×10^{-4} Pa. The shift in the NIST ion gauge inverse correction factor at 9×10^{-4} Pa was much larger than the shifts in the NIST SRG calibration ratios (relative standard deviations of 0.41 % and 0.83 % for the two SRGs), which supports the pressure independent correction of eq. (22). Further support for the approach taken regarding correcting for the pressure independent changes in the ion gauge characteristics is found by examining the standard deviations, $\sigma(a_{ijm})$ and $\sigma(S_{jm})$, of the calibrations at all NMIs at 9×10^{-4} Pa. For the two SRGs, the relative standard deviations were 0.9 %; for SI-404, the relative standard deviation was 1.7 %. It should be remembered that these standard deviations include both the difference between the NMIs and the shifts in the gauge constants.

Figure 7b shows the pressure-independent normalization in the form of the calibration ratio, K_{jm} for NIST. In the normalization, K_{jm} at 9×10^{-4} Pa is set equal to $\hat{p}_{jU} / \hat{p}_R$ from the SRGs. The normalization has the effect of increasing the apparent long-term response shifts in the ion gauge characteristics at the lower pressures. This same data is plotted in Fig. 8 in chronological progression with the calibration cycle on the *x*-axis, as curves of constant pressure. The calibration ratio at NIST shifted both upward and downward throughout the comparison.

Standard uncertainties in the predicted gauge reading, $u_c(p_{jm})$, are dominated by standard uncertainties in long-term shifts of the ion gauges for nearly all NMIs for pressures of 3×10^{-5} Pa and lower. At the higher pressures, u_{std} is comparable to or larger than u_{LTS} for NPL, NPLI, and KRISS. At 9×10^{-5} Pa and 3×10^{-4} Pa, u_{SRG} becomes comparable to other components for all NMIs. The Type A standard uncertainty is usually the smallest uncertainty component, except for NIST3.

Table 10. Results for ion gauge SI-404 for each cycle at each NMI, as a function of target pressure (P_T). Shown are ion gauge inverse correction factor (S_{jm}) and its relative Type A standard uncertainty ($u_A(S_{jm})/S_{jm}$), calibration ratio (K_{jm}), predicted gauge reading (p_{jm}), relative standard uncertainty contributions to $u_c(p_{jm})$, and $u_c(p_{jm})$. S_{jm} has been corrected for temperature deviation from 293.15 K and pressure deviation from target pressure. By definition, $K_{jm} = \hat{p}_{jU} / \hat{p}_R$ at 9×10^{-4} Pa.

NMI j Cycle m	P_T / Pa	S_{jm}	$u_A(S_{jm})$ / S_{jm}	K_{jm}	p_{jm} / Pa	Relative standard uncertainties on p_{jm}					$u_c(p_{jm})$ / Pa
						u_A	u_{std}	u_{SRG}	u_{LTS}	u_c	
NIST1	$3x10^{-6}$	1.3089	0.00118	0.9443	2.833E-06	0.00199	0.00540	0.00302	0.01876	0.01985	5.62E-08
	$9x10^{-6}$	1.3219	0.00108	0.9537	8.583E-06	0.00193	0.00330	0.00302	0.01274	0.01364	1.17E-07
	$3x10^{-5}$	1.3400	0.00104	0.9667	2.900E-05	0.00191	0.00210	0.00302	0.01098	0.01174	3.40E-07
	$9x10^{-5}$	1.3506	0.00132	0.9744	8.770E-05	0.00208	0.00200	0.00302	0.00553	0.00693	6.07E-07
	$3x10^{-4}$	1.3752	0.00111	0.9922	2.977E-04	0.00195	0.00170	0.00302	0.00260	0.00475	1.41E-06
	$9x10^{-4}$	1.3888	0.00160	**1.0019**	9.017E-04	0.00160	0.00170	---	---	---	---
NIST2	$3x10^{-6}$	1.3022	0.00140	0.9721	2.916E-06	0.00193	0.00540	0.00302	0.01876	0.01984	5.79E-08
	$9x10^{-6}$	1.3094	0.00105	0.9774	8.797E-06	0.00170	0.00330	0.00302	0.01274	0.01361	1.20E-07
	$3x10^{-5}$	1.3228	0.00084	0.9874	2.962E-05	0.00157	0.00210	0.00302	0.01098	0.01169	3.46E-07
	$9x10^{-5}$	1.3196	0.00159	0.9851	8.866E-05	0.00207	0.00200	0.00302	0.00553	0.00692	6.14E-07
	$3x10^{-4}$	1.3357	0.00107	0.9971	2.991E-04	0.00171	0.00170	0.00302	0.00260	0.00465	1.39E-06
	$9x10^{-4}$	1.3422	0.00133	**1.0019**	9.017E-04	0.00133	0.00170	---	---	---	---
NIST3	$3x10^{-6}$	1.2907	0.01465	0.9547	2.864E-06	0.01515	0.00540	0.00302	0.01876	0.02489	7.13E-08
	$9x10^{-6}$	1.3051	0.00847	0.9654	8.688E-06	0.00930	0.00330	0.00302	0.01274	0.01640	1.42E-07
	$3x10^{-5}$	1.3174	0.00258	0.9745	2.923E-05	0.00463	0.00210	0.00302	0.01098	0.01248	3.65E-07
	$9x10^{-5}$	1.3245	0.00167	0.9797	8.818E-05	0.00420	0.00200	0.00302	0.00553	0.00783	6.90E-07
	$3x10^{-4}$	1.3430	0.00077	0.9934	2.980E-04	0.00393	0.00170	0.00302	0.00260	0.00584	1.74E-06
	$9x10^{-4}$	1.3545	0.00385	**1.0019**	9.017E-04	0.00385	0.00170	---	---	---	---
NIST4	$3x10^{-6}$	1.3082	0.00194	0.9753	2.926E-06	0.00235	0.00540	0.00302	0.01876	0.01989	5.82E-08
	$9x10^{-6}$	1.3020	0.00177	0.9706	8.735E-06	0.00221	0.00330	0.00302	0.01274	0.01368	1.20E-07
	$3x10^{-5}$	1.3148	0.00118	0.9801	2.940E-05	0.00178	0.00210	0.00302	0.01098	0.01172	3.45E-07
	$9x10^{-5}$	1.3158	0.00166	0.9809	8.828E-05	0.00212	0.00200	0.00302	0.00553	0.00694	6.13E-07
	$3x10^{-4}$	1.3332	0.00190	0.9939	2.982E-04	0.00231	0.00170	0.00302	0.00260	0.00491	1.46E-06
	$9x10^{-4}$	1.3440	0.00133	**1.0019**	9.017E-04	0.00133	0.00170	---	---	---	---
PTB1	$3x10^{-6}$	1.3368	0.00276	0.9476	2.843E-06	0.00324	0.00200	0.00448	0.01876	0.01966	5.59E-08
	$9x10^{-6}$	1.3330	0.00161	0.9449	8.504E-06	0.00234	0.00200	0.00448	0.01274	0.01385	1.18E-07
	$3x10^{-5}$	1.3409	0.00123	0.9505	2.851E-05	0.00210	0.00200	0.00448	0.01098	0.01221	3.48E-07
	$9x10^{-5}$	1.3463	0.00155	0.9544	8.589E-05	0.00230	0.00200	0.00448	0.00553	0.00774	6.65E-07
	$3x10^{-4}$	1.3797	0.00215	0.9780	2.934E-04	0.00274	0.00100	0.00448	0.00260	0.00595	1.74E-06
	$9x10^{-4}$	1.3935	0.00170	**0.9878**	8.890E-04	0.00170	0.00100	---	---	---	---
	$3x10^{-3}$	1.4126	0.00493	1.0014	3.004E-03	0.00521	0.00110	---	---	---	---
	$9x10^{-3}$	1.3890	0.00272	0.9846	8.862E-03	0.00321	0.00140	---	---	---	---

Table 10 (continued). Results for ion gauge SI-404 for each cycle at each NMI, as a function of target pressure (P_T).

NMI j Cycle m	P_T / Pa	S_{jm}	$u_A(S_{jm})$ / S_{jm}	K_{jm}	p_{jm} / Pa	Relative standard uncertainties on p_{jm}					$u_c(p_{jm})$ / Pa
						u_A	u_{std}	u_{SRG}	u_{LTS}	u_c	
PTB2	3x10^{-6}	1.3329	0.00312	0.9438	2.832E-06	0.00352	0.00200	0.00448	0.01876	0.01971	5.58E-08
	9x10^{-6}	1.3314	0.00448	0.9428	8.485E-06	0.00477	0.00200	0.00448	0.01274	0.01446	1.23E-07
	3x10^{-5}	1.3433	0.00284	0.9512	2.854E-05	0.00328	0.00200	0.00448	0.01098	0.01247	3.56E-07
	9x10^{-5}	1.3460	0.00364	0.9531	8.578E-05	0.00399	0.00200	0.00448	0.00553	0.00840	7.21E-07
	3x10^{-4}	1.3806	0.00427	0.9776	2.933E-04	0.00457	0.00100	0.00448	0.00260	0.00698	2.05E-06
	9x10^{-4}	1.3950	0.00163	**0.9878**	8.890E-04	0.00163	0.00100	---------	---------	---------	---------
	3x10^{-3}	1.4168	0.00130	1.0032	3.010E-03	0.00209	0.00110	---------	---------	---------	---------
	9x10^{-3}	1.3893	0.00169	0.9838	8.854E-03	0.00235	0.00140	---------	---------	---------	---------
NPL	9x10^{-7}	1.3217	0.00262	0.9821	8.839E-07	0.00430	0.00760	---------	---------	---------	---------
	3x10^{-6}	1.3251	0.00233	0.9846	2.954E-06	0.00413	0.00550	0.00601	0.01876	0.02086	6.16E-08
	9x10^{-6}	1.3215	0.00184	0.9819	8.837E-06	0.00387	0.00480	0.00601	0.01274	0.01538	1.36E-07
	3x10^{-5}	1.3250	0.00107	0.9845	2.954E-05	0.00357	0.00460	0.00601	0.01098	0.01381	4.08E-07
	9x10^{-5}	1.3311	0.00085	0.9891	8.902E-05	0.00351	0.00460	0.00601	0.00553	0.01001	8.91E-07
	3x10^{-4}	1.3323	0.00230	0.9900	2.970E-04	0.00412	0.00360	0.00601	0.00260	0.00853	2.53E-06
	9x10^{-4}	1.3432	0.00341	**0.9980**	8.982E-04	0.00341	0.00350	---------	---------	---------	---------
NPLI	3x10^{-6}	1.2864	0.00163	0.9680	2.904E-06	0.00364	0.00860	0.00604	0.01876	0.02180	6.33E-08
	9x10^{-6}	1.2846	0.00101	0.9667	8.700E-06	0.00341	0.00780	0.00604	0.01274	0.01647	1.43E-07
	3x10^{-5}	1.2961	0.00217	0.9753	2.926E-05	0.00391	0.00750	0.00604	0.01098	0.01512	4.42E-07
	9x10^{-5}	1.3095	0.00321	0.9854	8.869E-05	0.00457	0.00820	0.00604	0.00553	0.01245	1.10E-06
	3x10^{-4}	1.3301	0.00284	1.0009	3.003E-04	0.00431	0.00830	0.00604	0.00260	0.01143	3.43E-06
	9x10^{-4}	1.3325	0.00325	**1.0027**	9.024E-04	0.00325	0.00760	---------	---------	---------	---------
KRISS	3x10^{-6}	1.3197	0.00133	0.9750	2.925E-06	0.00169	0.00671	0.00634	0.01876	0.02097	6.13E-08
	9x10^{-6}	1.3034	0.00116	0.9629	8.666E-06	0.00157	0.00470	0.00634	0.01274	0.01507	1.31E-07
	3x10^{-5}	1.3097	0.00144	0.9675	2.903E-05	0.00178	0.00537	0.00634	0.01098	0.01389	4.03E-07
	9x10^{-5}	1.3146	0.00122	0.9711	8.740E-05	0.00161	0.00686	0.00634	0.00553	0.01097	9.59E-07
	3x10^{-4}	1.3314	0.00071	0.9836	2.951E-04	0.00127	0.00540	0.00634	0.00260	0.00881	2.60E-06
	9x10^{-4}	1.3642	0.00105	**1.0078**	9.070E-04	0.00105	0.00469	---------	---------	---------	---------

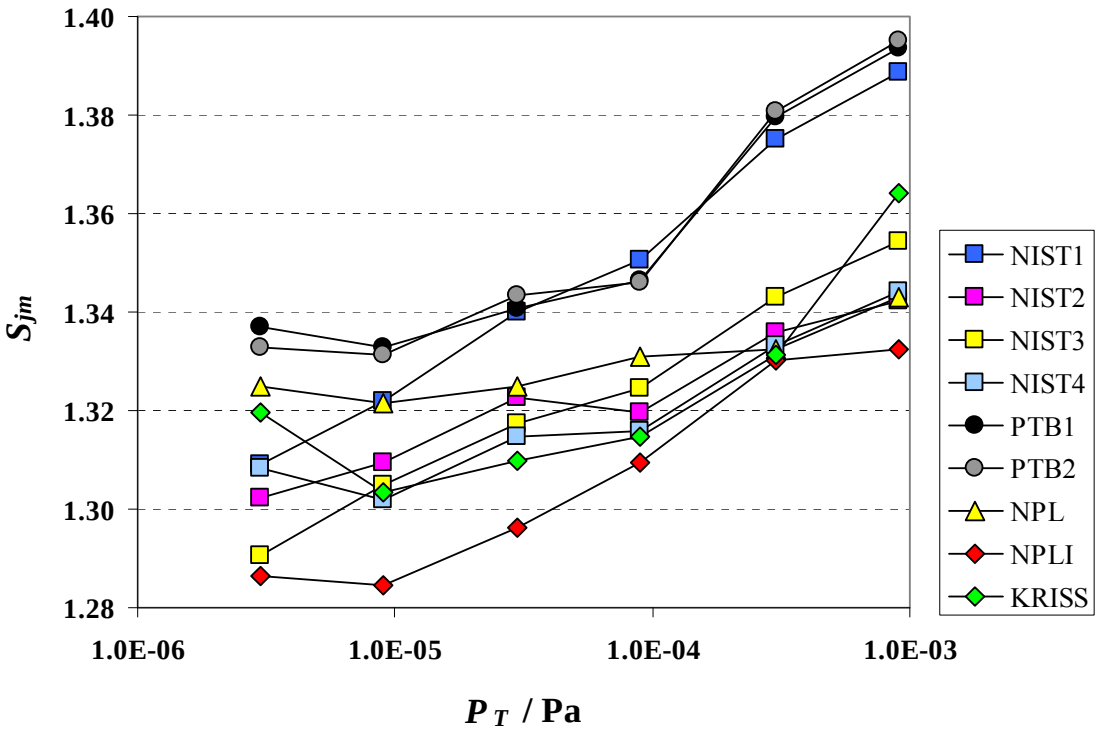

Figure 6. Average ion gauge inverse correction factor, S_{jm}, for gauge SI-404 as a function of target pressure, P_T, for each calibration cycle at each NMI. By definition, S_{jm} is not corrected for pressure independent shifts at 9×10^{-4} Pa.

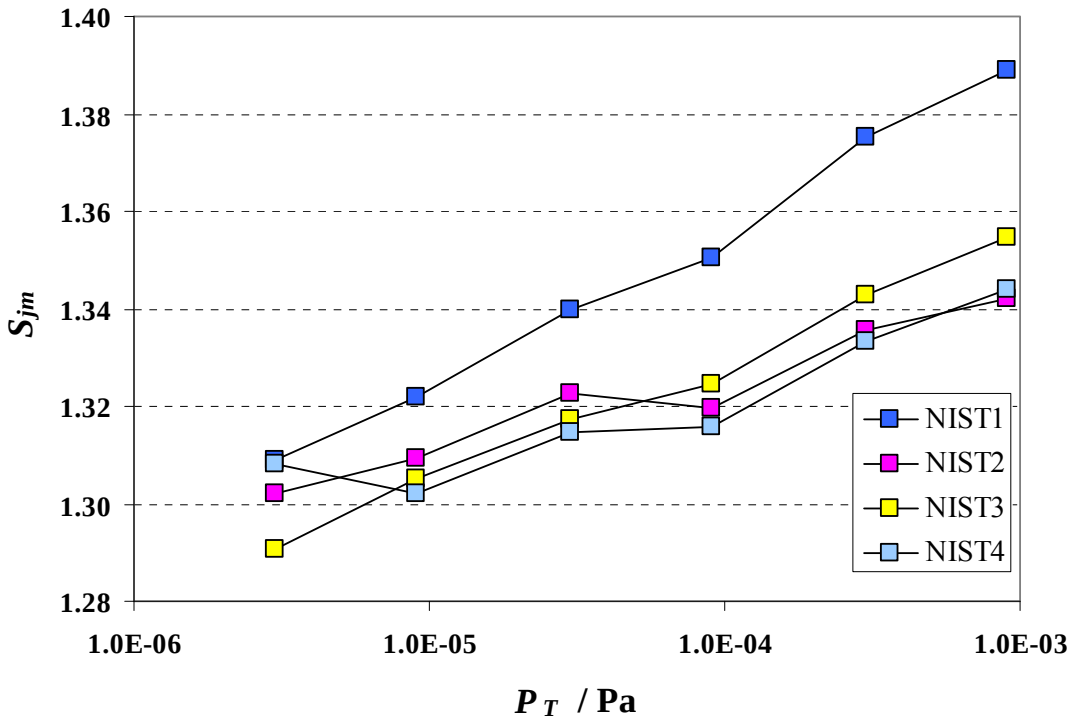

Figure 7a. Average ion gauge inverse correction factor, S_{jm}, for gauge SI-404 as a function of target pressure, P_T, for the four NIST calibration cycles.

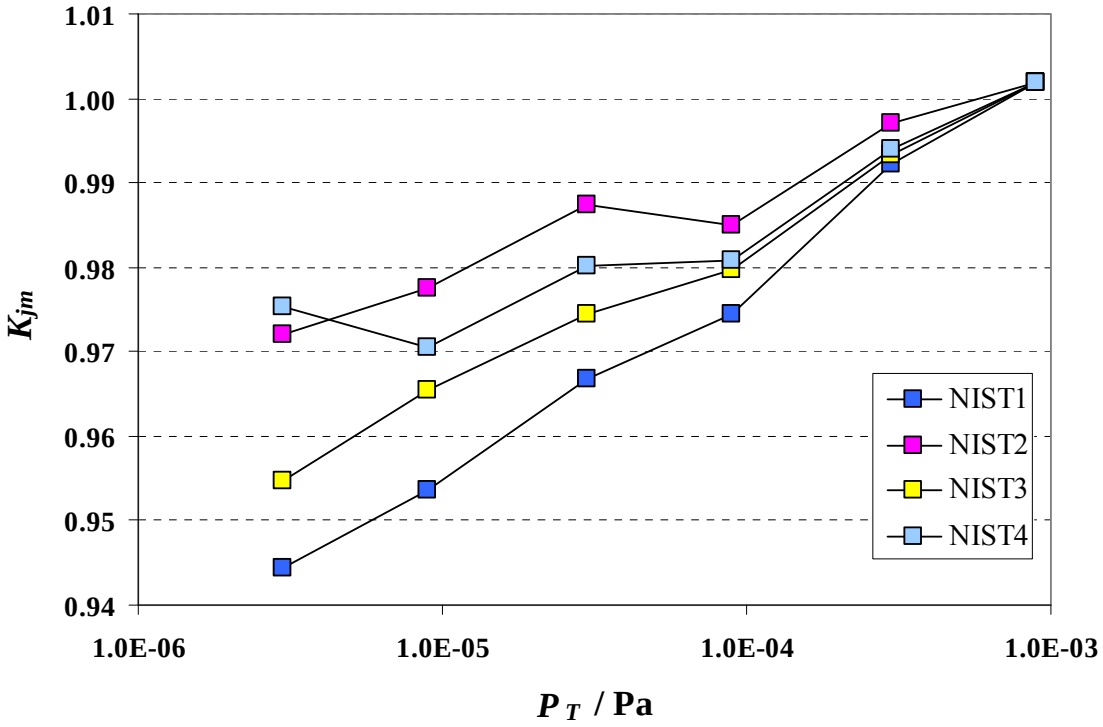

Figure 7b. Ion gauge calibration ratio, K_{jm}, for gauge SI-404 as a function of target pressure, P_T, for the four NIST calibration cycles. Normalization sets K_{jm} equal to pressure ratio, $\hat{p}_{jU} / \hat{p}_R$, determined from SRGs at 9×10^{-4} Pa.

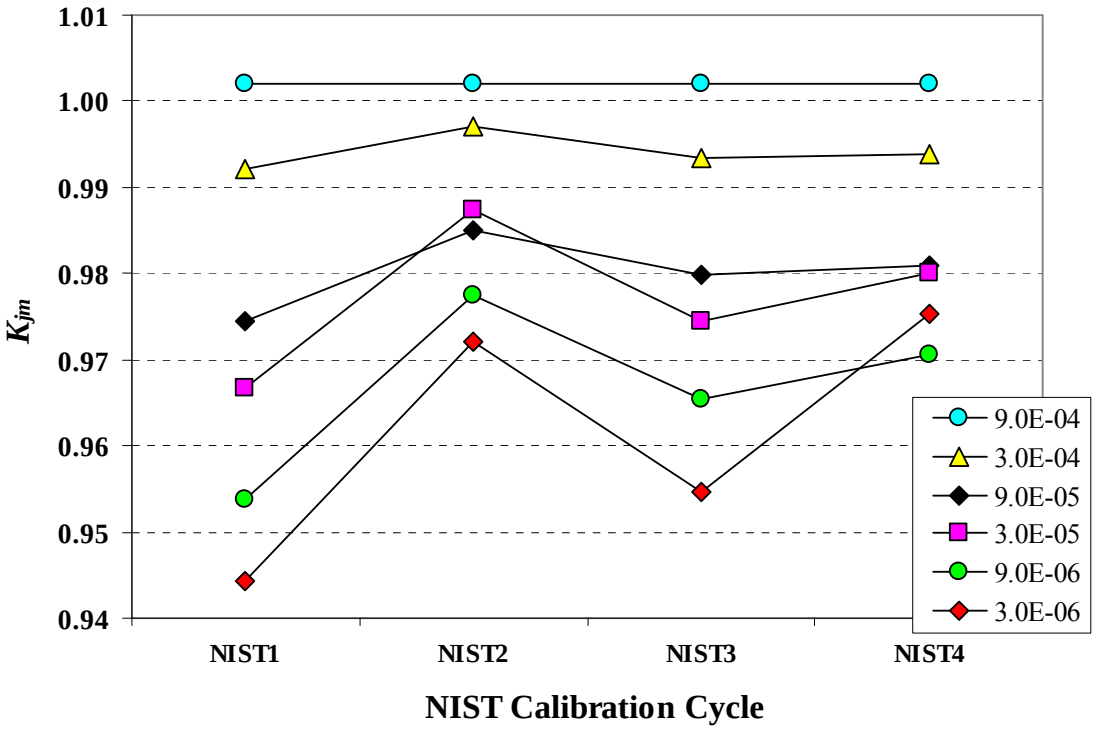

Figure 8. Ion gauge calibration ratio, K_{jm}, for the four NIST calibration cycles in chronological order, at target pressures, P_T, from 3×10^{-6} Pa to 9×10^{-4} Pa. Normalization sets K_{jm} equal to to pressure ratio, $\hat{p}_{jU} / \hat{p}_R$ determined from SRGs at 9×10^{-4} Pa

The results of the mean gauge pressure reading (p_{jU}) from the ion gauge calibrations, for the five NMIs at the target pressures of the comparison, are summarized in Table 11. Except for PTB and NIST, these will be the same as those for p_{jm} in Table 10. Listed are the mean gauge reading (p_{jU}), its standard uncertainty ($u(p_{jU})$), and the relative standard uncertainty ($u(p_{jU})/p_{jU}$). These results are plotted in Fig. 9 as the ratio p_{jU}/P_T as a function of P_T, with the result at 9×10^{-4} anchored to the mean gauge pressure from the SRGs. There is increasing relative agreement of the mean gauge pressure to the target pressure as the pressure increases, which was previously seen in the ion gauge inverse correction factor (Fig. 6). This variation with pressure is a property of the specific ion gauge used in the comparison, and will be accounted for in calculating the KCRV and the scaling factor. For clarity, relative standard uncertainties are not plotted; these uncertainties range from a maximum of 2.2 % at 9×10^{-6} Pa to a minimum of 0.4 % at 3×10^{-4} Pa. The PTB mean gauge reading is consistently lower than the other NMIs, ranging from 0.6 % to 2.1 % below the next lowest reading of the other NMIs. The normalization to the SRG result at 9×10^{-4} Pa contributes to this shift.

7.3 Degrees of equivalence of the primary standards

The choice of the KCRV, the calculation of its uncertainty, the calculation of the differences between each NMI and the KCRV, and the uncertainty of those differences are explained in Appendix A. Here we summarize the results of applying that model to the data.

The degree of equivalence of the NMI primary standards to the reference value is summarized in Table 12. Table 12 lists the corrected mean gauge pressure reading (p_j); the difference (d_j) between p_j and the KCRV (p_R); the uncertainty of those parameters; and the difference divided by its expanded uncertainty ($d_j/U(d_j)$). Shaded cells indicate results where there is a lack of equivalence at the k=2 level. Recall that through the scaling factor f_C, p_j is defined such that when the KCRV is calculated, the KCRV numerically equals the target pressure. Figure 10 is a plot of the relative difference to the KCRV (d_j/p_R) as a function of pressure for the five NMIs. For clarity, uncertainties are not plotted. The PTB corrected mean gauge reading is 1.4 % to 2.8 % below the KCRV. The results for the degree of equivalence to the reference value are shown graphically in Figs. 11 to 16. Each figure shows one pressure, with d_j/p_R plotted for each NMI and the expanded relative uncertainty $U(d_j)/p_R$ shown as error bars. When the error bars cross the x-axis there is equivalence to the reference value at k=2. The primary standards of NIST, NPL, NPLI, and KRISS are equivalent to p_R at all pressures. PTB's primary standard is equivalent at 3×10^{-6} Pa only; however it is only marginally non-equivalent at 9×10^{-6} Pa and 3×10^{-4} Pa ($d_{PTB}/U(d_{PTB}) = -1.059$ and $= -1.028$). The results for all NMIs and all pressures are presented in Fig. 17. Here, the difference d_j is normalized to the expanded uncertainty, $U(d_j)$. Values of $d_j/U(d_j)$ between −1 and +1 indicate equivalence to the KCRV.

The degree of equivalence between NMIs is summarized in Tables 13a and 13b. $d_{jj'}$ is the pair-wise difference in corrected mean gauge pressure reading between the NMIs, and $U(d_{jj'})$ is the expanded uncertainty of the difference. Table 13a lists the parameters

Table 11. Summary of results at target pressures from 3×10^{-6} Pa to 3×10^{-4} Pa based on calibrations of ion gauge SI-404. Listed are mean gauge pressure reading (p_{jU}), uncertainty in mean gauge pressure reading $u(p_{jU})$, and its relative uncertainty $u(p_{jU})/p_{jU}$.

P_T / Pa	NMI j	p_{jU} / Pa	$u(p_{jU})$ / Pa	$u(p_{jU})$ / p_{jU}
$3x10^{-6}$	NIST	2.885E-06	3.43E-08	0.0119
	PTB	2.837E-06	4.07E-08	0.0143
	NPL	2.954E-06	6.16E-08	0.0209
	NPLI	2.904E-06	6.33E-08	0.0218
	KRISS	2.925E-06	6.13E-08	0.0210
$9x10^{-6}$	NIST	8.701E-06	7.11E-08	0.0082
	PTB	8.495E-06	9.00E-08	0.0106
	NPL	8.837E-06	1.36E-07	0.0154
	NPLI	8.700E-06	1.43E-07	0.0165
	KRISS	8.666E-06	1.31E-07	0.0151
$3x10^{-5}$	NIST	2.932E-05	1.98E-07	0.0068
	PTB	2.853E-05	2.68E-07	0.0094
	NPL	2.954E-05	4.08E-07	0.0138
	NPLI	2.926E-05	4.42E-07	0.0151
	KRISS	2.903E-05	4.03E-07	0.0139
$9x10^{-5}$	NIST	8.820E-05	4.20E-07	0.0048
	PTB	8.584E-05	5.74E-07	0.0067
	NPL	8.902E-05	8.91E-07	0.0100
	NPLI	8.869E-05	1.10E-06	0.0125
	KRISS	8.740E-05	9.59E-07	0.0110
$3x10^{-4}$	NIST	2.982E-04	1.17E-06	0.0039
	PTB	2.933E-04	1.65E-06	0.0056
	NPL	2.970E-04	2.53E-06	0.0085
	NPLI	3.003E-04	3.43E-06	0.0114
	KRISS	2.951E-04	2.60E-06	0.0088

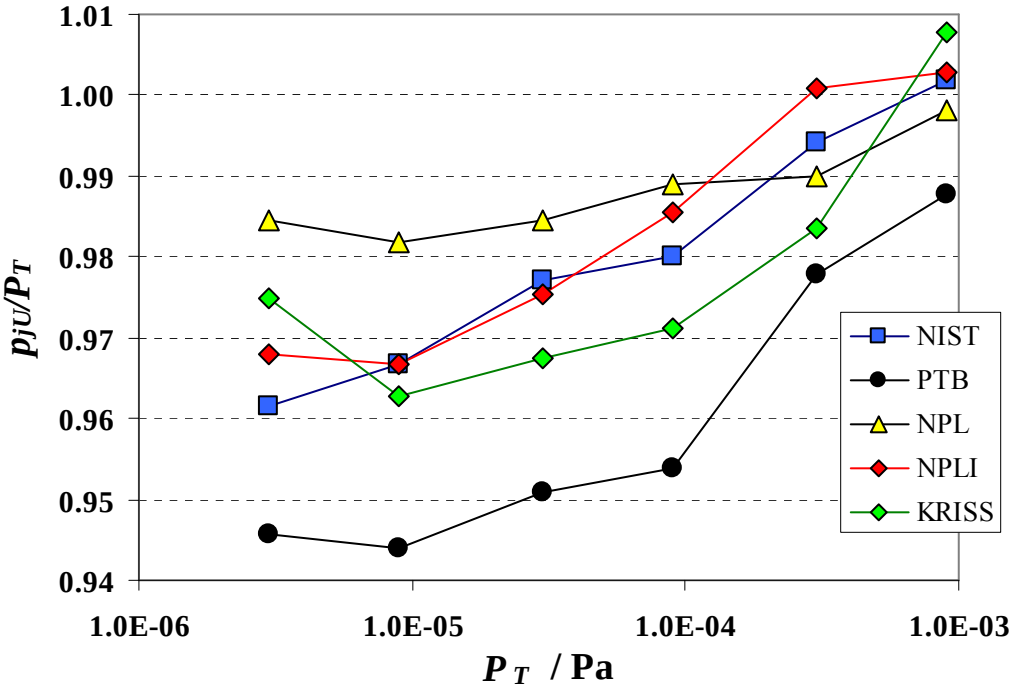

Figure 9. Relative mean gauge pressure reading (p_{jU}/P_T) using ion gauge SI-404, as a function of target pressure, for each NMI. Values at 9×10^{-4} Pa set by scaling to SRG result.

Table 12. Summary of results at target pressures from 3×10^{-6} Pa to 9×10^{-4} Pa. Listed are corrected mean gauge pressure reading (p_j), difference (d_j) between p_j and reference pressure (p_R), and associated standard uncertainties. $U(d_j) = 2u(d_j)$. Shaded cells indicate results where $|d_j|$ exceeds $U(d_j)$.

P_T / Pa	NMI j	p_j / Pa	$u(p_j)$ / Pa	d_j / Pa	$u(d_j)$ / Pa	d_j/p_R	$d_j / U(d_j)$
$3x10^{-6}$	NIST	2.967E-06	3.53E-08	-3.30E-08	3.83E-08	-0.0110	-0.431
	PTB	2.918E-06	4.19E-08	-8.19E-08	5.09E-08	-0.0273	-0.804
	NPL	3.038E-06	6.34E-08	3.79E-08	5.34E-08	0.0126	0.355
	NPLI	2.987E-06	6.51E-08	-1.33E-08	5.44E-08	-0.0044	-0.122
	KRISS	3.008E-06	6.31E-08	8.29E-09	5.32E-08	0.0028	0.078
$9x10^{-6}$	NIST	8.974E-06	7.33E-08	-2.58E-08	8.22E-08	-0.0029	-0.157
	PTB	8.762E-06	9.29E-08	-2.38E-07	1.13E-07	-0.0265	-1.059
	NPL	9.114E-06	1.40E-07	1.14E-07	1.18E-07	0.0127	0.486
	NPLI	8.973E-06	1.48E-07	-2.67E-08	1.22E-07	-0.0030	-0.109
	KRISS	8.938E-06	1.35E-07	-6.20E-08	1.15E-07	-0.0069	-0.271
$3x10^{-5}$	NIST	3.003E-05	2.03E-07	3.27E-08	2.40E-07	0.0011	0.068
	PTB	2.922E-05	2.74E-07	-7.77E-07	3.35E-07	-0.0259	-1.160
	NPL	3.026E-05	4.18E-07	2.57E-07	3.53E-07	0.0086	0.365
	NPLI	2.997E-05	4.53E-07	-2.60E-08	3.74E-07	-0.0009	-0.035
	KRISS	2.974E-05	4.13E-07	-2.64E-07	3.50E-07	-0.0088	-0.378
$9x10^{-5}$	NIST	8.987E-05	4.28E-07	-1.26E-07	5.42E-07	-0.0014	-0.117
	PTB	8.746E-05	5.85E-07	-2.54E-06	7.37E-07	-0.0282	-1.720
	NPL	9.070E-05	9.08E-07	7.03E-07	7.83E-07	0.0078	0.449
	NPLI	9.037E-05	1.13E-06	3.66E-07	9.14E-07	0.0041	0.200
	KRISS	8.906E-05	9.77E-07	-9.43E-07	8.24E-07	-0.0105	-0.572
$3x10^{-4}$	NIST	3.006E-04	1.18E-06	6.07E-07	1.54E-06	0.0020	0.197
	PTB	2.957E-04	1.66E-06	-4.33E-06	2.11E-06	-0.0144	-1.028
	NPL	2.993E-04	2.55E-06	-6.57E-07	2.22E-06	-0.0022	-0.148
	NPLI	3.026E-04	3.46E-06	2.64E-06	2.77E-06	0.0088	0.476
	KRISS	2.974E-04	2.62E-06	-2.59E-06	2.26E-06	-0.0086	-0.572
$9x10^{-4}$	NIST	8.994E-04	3.12E-06	-6.16E-07	3.98E-06	-0.0007	-0.077
	PTB	8.867E-04	4.10E-06	-1.33E-05	5.27E-06	-0.0148	-1.260
	NPL	8.959E-04	6.23E-06	-4.13E-06	5.51E-06	-0.0046	-0.375
	NPLI	9.001E-04	8.74E-06	9.54E-08	7.01E-06	0.0001	0.007
	KRISS	9.046E-04	7.13E-06	4.65E-06	6.03E-06	0.0052	0.385

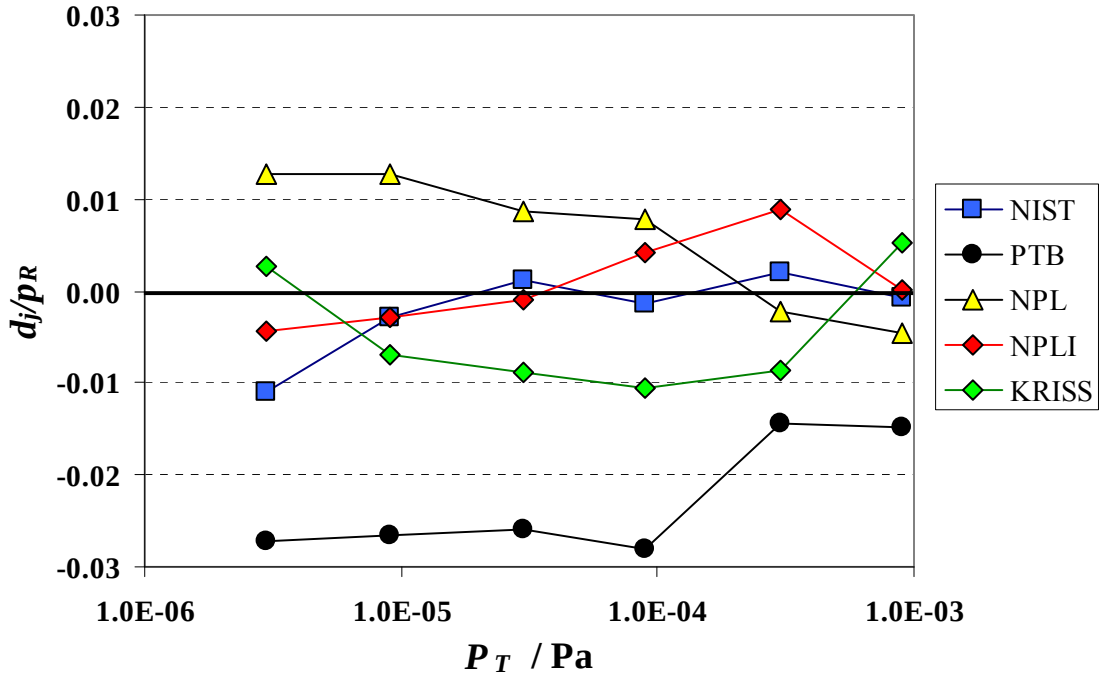

Figure 10. Relative difference (d_j/p_R) between corrected mean gauge pressure reading (p_j) and reference pressure (p_R), for target pressures from 3×10^{-6} Pa to 9×10^{-4} Pa for all NMIs. Results at 9×10^{-4} Pa based on SRGs; results at lower pressures based on SI-404 and scaling to the SRG result.

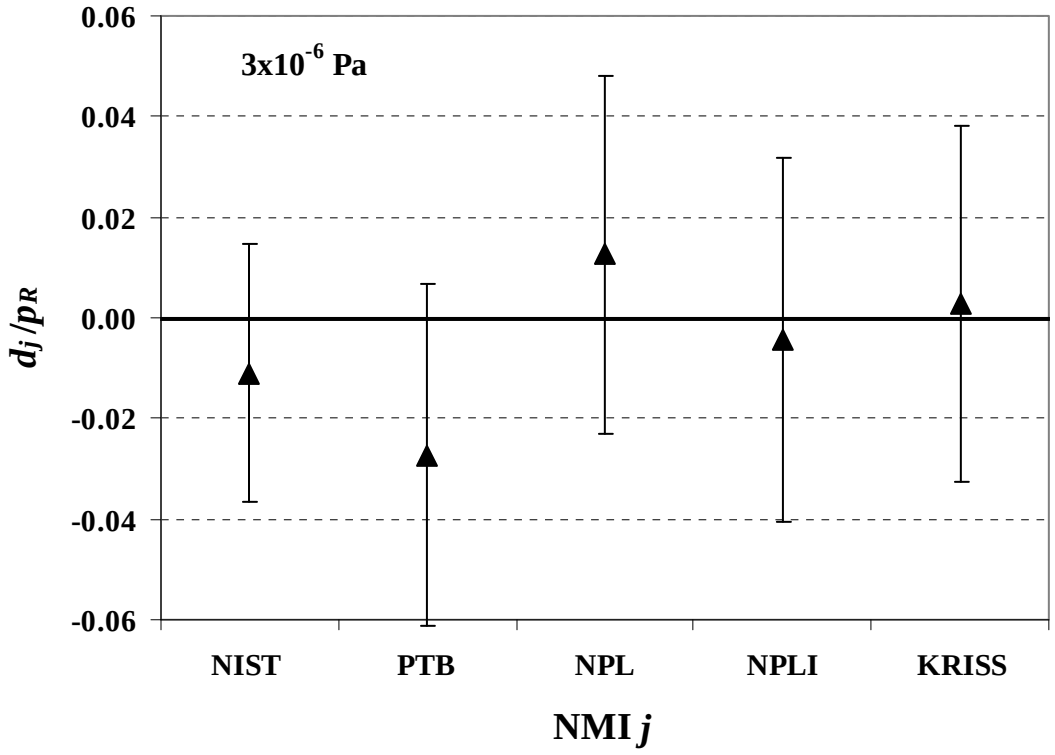

Figure 11. Degree of equivalence at 3×10^{-6} Pa for each NMI. Plotted is relative difference (d_j/p_R) of corrected mean gauge pressure reading (p_j) from reference value (p_R), with expanded (k=2) uncertainty in relative difference shown as error bars. When error bars cross x-axis, there is equivalence to the reference value.

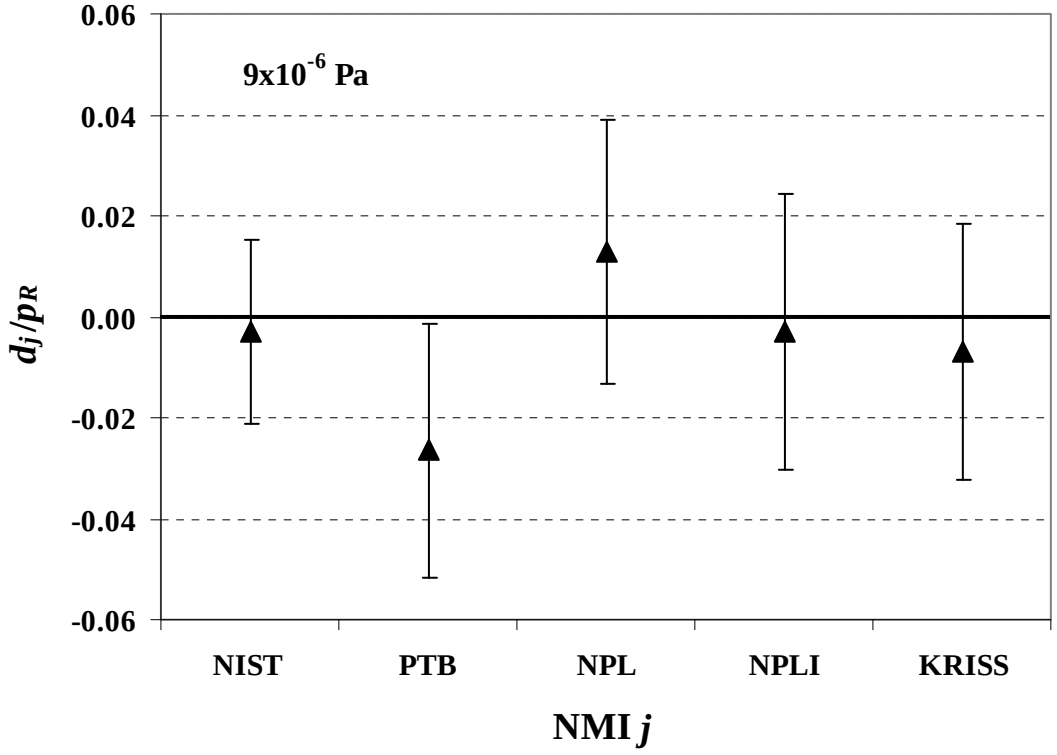

Figure 12. Degree of equivalence at 9×10^{-6} Pa for each NMI. Plotted is relative difference (d_j/p_R) of corrected mean gauge pressure reading (p_j) from reference value (p_R), with expanded (k=2) uncertainty in relative difference shown as error bars. When error bars cross x-axis, there is equivalence to the reference value.

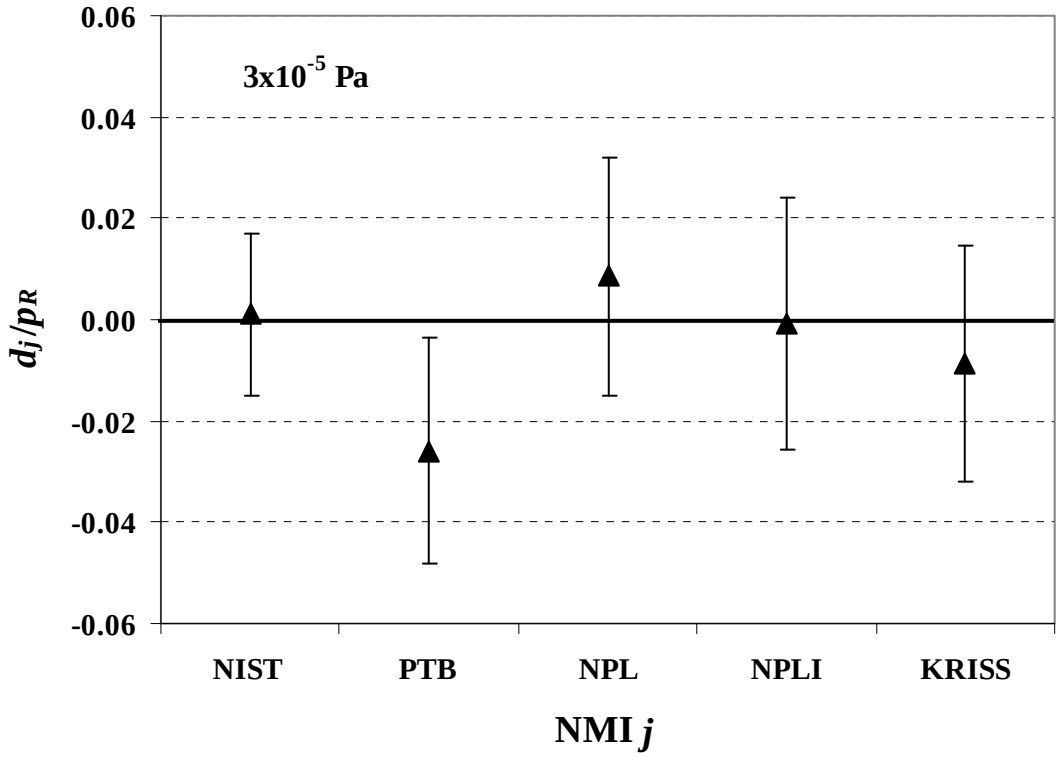

Figure 13. Degree of equivalence at 3×10^{-5} Pa for each NMI. Plotted is relative difference (d_j/p_R) of corrected mean gauge pressure reading (p_j) from reference value (p_R), with expanded (k=2) uncertainty in relative difference shown as error bars. When error bars cross x-axis, there is equivalence to the reference value.

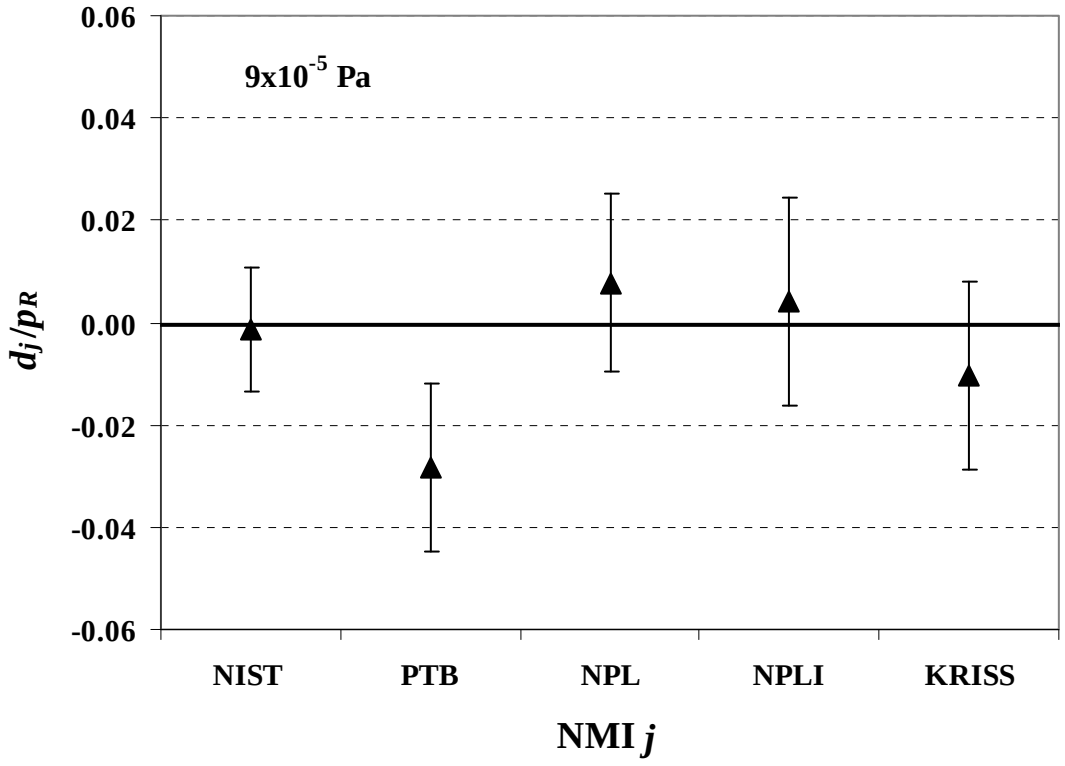

Figure 14. Degree of equivalence at 9×10^{-5} Pa for each NMI. Plotted is relative difference (d_j/p_R) of corrected mean gauge pressure reading (p_j) from reference value (p_R), with expanded (k=2) uncertainty in relative difference shown as error bars. When error bars cross x-axis, there is equivalence to the reference value.

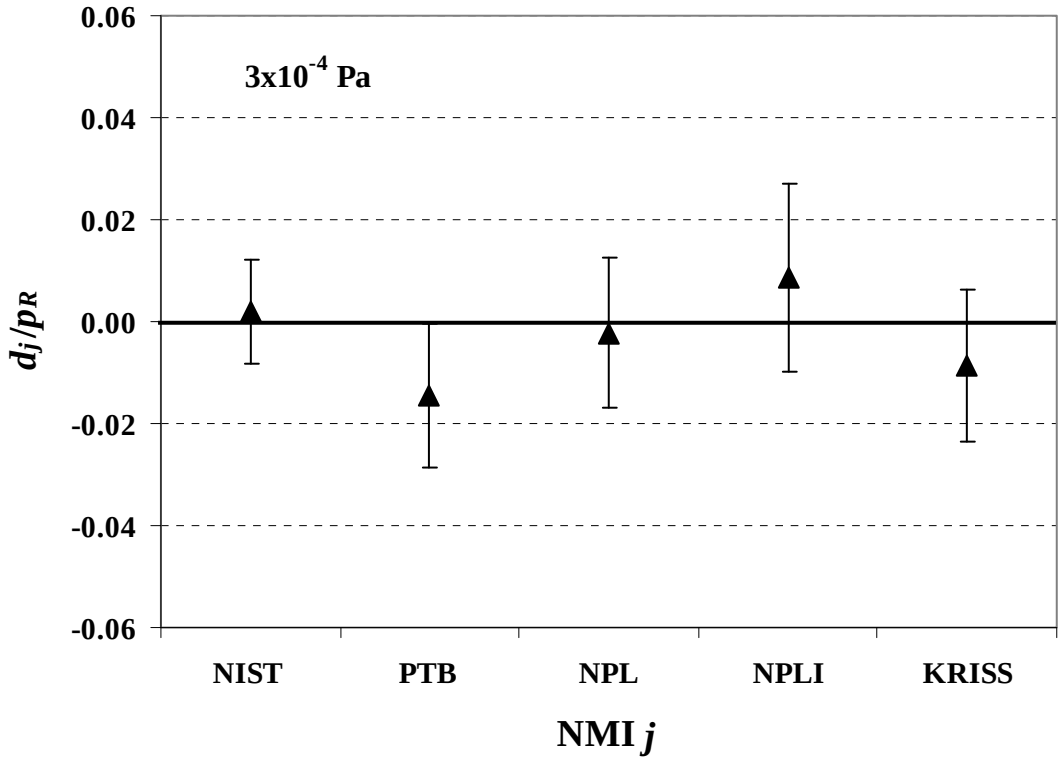

Figure 15. Degree of equivalence at 3×10^{-4} Pa for each NMI. Plotted is relative difference (d_j/p_R) of corrected mean gauge pressure reading (p_j) from reference value (p_R), with expanded (k=2) uncertainty in relative difference shown as error bars. When error bars cross x-axis, there is equivalence to the reference value.

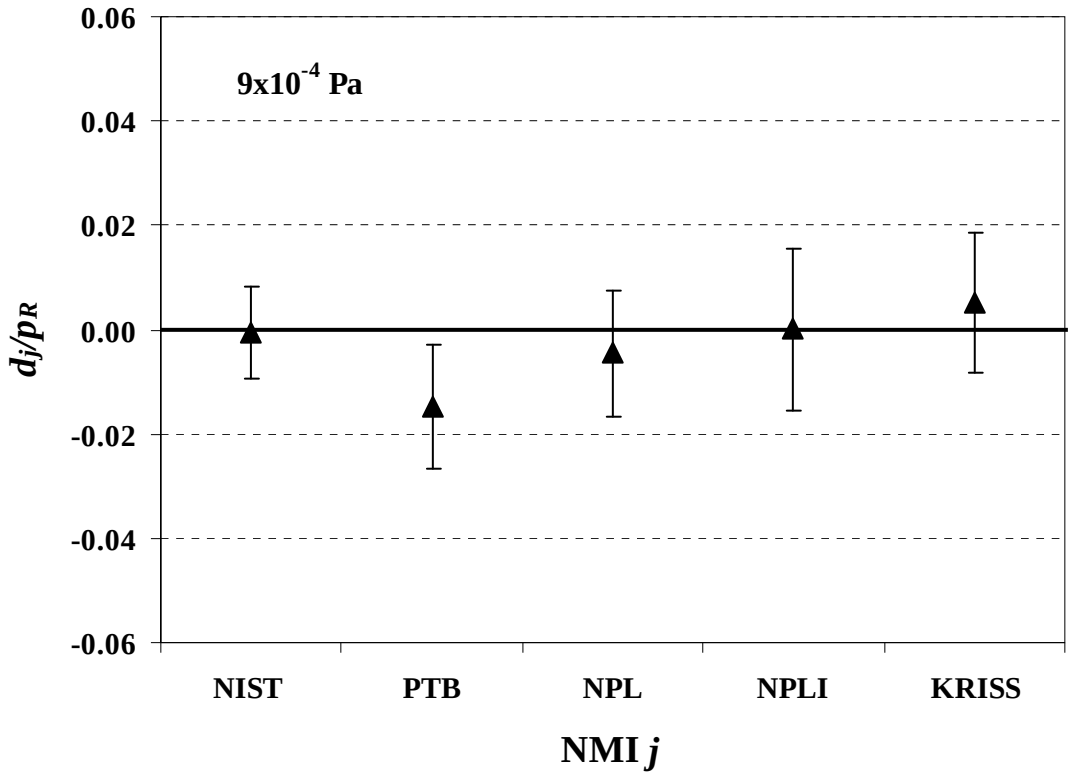

Figure 16. Degree of equivalence at 9×10^{-4} Pa for each NMI. Plotted is relative difference (d_j/p_R) of corrected mean gauge pressure reading (p_j) from reference value (p_R), with expanded (k=2) uncertainty in relative difference shown as error bars. When error bars cross x-axis, there is equivalence to the reference value.

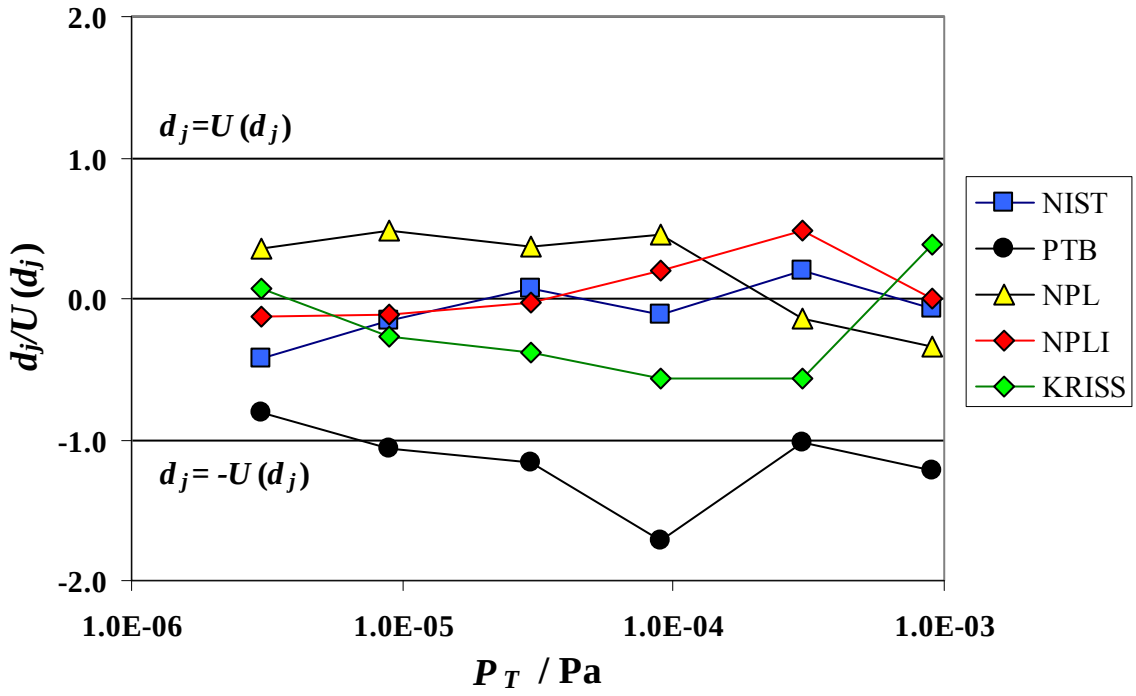

Figure 17. Summary of results for the degree of equivalence for each NMI with respect to the key comparison reference value, expressed as $d_j/U(d_j)$. When $|d_j/U(d_j)| \leq 1.0$ there is equivalence at k=2 expanded uncertainty.

Table 13a. Summary of degree of equivalence to reference value (d_j, $U(d_j)$) and pair-wise degree of equivalence between the participants ($d_{jj'}$, $U(d_{jj'})$). Expanded uncertainty U given at k=2. Shaded cells indicate results where $|d_j|$ exceeds $U(d_j)$ or $|d_{jj'}|$ exceeds $U(d_{jj'})$.

				NMI$_{j'}$ = NIST		NMI$_{j'}$ = PTB		NMI$_{j'}$ = NPL		NMI$_{j'}$ = NPLI		NMI$_{j'}$ = KRISS	
P_T / Pa	NMI$_j$	d_j / Pa	$U(d_j)$ / Pa	$d_{jj'}$ / Pa	$U(d_{jj'})$ / Pa	$d_{jj'}$ / Pa	$U(d_{jj'})$ / Pa	$d_{jj'}$ / Pa	$U(d_{jj'})$ / Pa	$d_{jj'}$ / Pa	$U(d_{jj'})$ / Pa	$d_{jj'}$ / Pa	$U(d_{jj'})$ / Pa
	NIST	-3.30E-08	7.66E-08			4.89E-08	1.09E-07	-7.09E-08	1.45E-07	-1.97E-08	1.48E-07	-4.13E-08	1.45E-07
	PTB	-8.19E-08	1.02E-07	-4.89E-08	1.09E-07			-1.20E-07	1.52E-07	-6.86E-08	1.55E-07	-9.02E-08	1.51E-07
3x10^{-6}	NPL	3.79E-08	1.07E-07	7.09E-08	1.45E-07	1.20E-07	1.52E-07			5.12E-08	1.82E-07	2.96E-08	1.79E-07
	NPLI	-1.33E-08	1.09E-07	1.97E-08	1.48E-07	6.86E-08	1.55E-07	-5.12E-08	1.82E-07			-2.15E-08	1.81E-07
	KRISS	8.29E-09	1.06E-07	4.13E-08	1.45E-07	9.02E-08	1.51E-07	-2.96E-08	1.79E-07	2.15E-08	1.81E-07		
	NIST	-2.58E-08	1.64E-07			2.13E-07	2.37E-07	-1.40E-07	3.16E-07	8.86E-10	3.30E-07	3.62E-08	3.07E-07
	PTB	-2.38E-07	2.25E-07	-2.13E-07	2.37E-07			-3.53E-07	3.36E-07	-2.12E-07	3.49E-07	-1.76E-07	3.27E-07
9x10^{-6}	NPL	1.14E-07	2.36E-07	1.40E-07	3.16E-07	3.53E-07	3.36E-07			1.41E-07	4.07E-07	1.76E-07	3.89E-07
	NPLI	-2.67E-08	2.45E-07	-8.86E-10	3.30E-07	2.12E-07	3.49E-07	-1.41E-07	4.07E-07			3.53E-08	4.00E-07
	KRISS	-6.20E-08	2.29E-07	-3.62E-08	3.07E-07	1.76E-07	3.27E-07	-1.76E-07	3.89E-07	-3.53E-08	4.00E-07		
	NIST	3.27E-08	4.80E-07			8.10E-07	6.83E-07	-2.25E-07	9.29E-07	5.87E-08	9.93E-07	2.97E-07	9.20E-07
	PTB	-7.77E-07	6.70E-07	-8.10E-07	6.83E-07			-1.03E-06	1.00E-06	-7.51E-07	1.06E-06	-5.13E-07	9.92E-07
3x10^{-5}	NPL	2.57E-07	7.05E-07	2.25E-07	9.29E-07	1.03E-06	1.00E-06			2.83E-07	1.23E-06	5.21E-07	1.17E-06
	NPLI	-2.60E-08	7.47E-07	-5.87E-08	9.93E-07	7.51E-07	1.06E-06	-2.83E-07	1.23E-06			2.38E-07	1.23E-06
	KRISS	-2.64E-07	6.99E-07	-2.97E-07	9.20E-07	5.13E-07	9.92E-07	-5.21E-07	1.17E-06	-2.38E-07	1.23E-06		
	NIST	-1.26E-07	1.08E-06			2.41E-06	1.45E-06	-8.29E-07	2.01E-06	-4.92E-07	2.41E-06	8.16E-07	2.13E-06
	PTB	-2.54E-06	1.47E-06	-2.41E-06	1.45E-06			-3.24E-06	2.16E-06	-2.90E-06	2.54E-06	-1.59E-06	2.28E-06
9x10^{-5}	NPL	7.03E-07	1.57E-06	8.29E-07	2.01E-06	3.24E-06	2.16E-06			3.37E-07	2.89E-06	1.65E-06	2.67E-06
	NPLI	3.66E-07	1.83E-06	4.92E-07	2.41E-06	2.90E-06	2.54E-06	-3.37E-07	2.89E-06			1.31E-06	2.98E-06
	KRISS	-9.43E-07	1.65E-06	-8.16E-07	2.13E-06	1.59E-06	2.28E-06	-1.65E-06	2.67E-06	-1.31E-06	2.98E-06		
	NIST	6.07E-07	3.08E-06			4.93E-06	4.08E-06	1.26E-06	5.63E-06	-2.03E-06	7.31E-06	3.19E-06	5.75E-06
	PTB	-4.33E-06	4.21E-06	-4.93E-06	4.08E-06			-3.67E-06	6.09E-06	-6.96E-06	7.68E-06	-1.74E-06	6.21E-06
3x10^{-4}	NPL	-6.57E-07	4.44E-06	-1.26E-06	5.63E-06	3.67E-06	6.09E-06			-3.29E-06	8.60E-06	1.93E-06	7.32E-06
	NPLI	2.64E-06	5.53E-06	2.03E-06	7.31E-06	6.96E-06	7.68E-06	3.29E-06	8.60E-06			5.22E-06	8.68E-06
	KRISS	-2.59E-06	4.52E-06	-3.19E-06	5.75E-06	1.74E-06	6.21E-06	-1.93E-06	7.32E-06	-5.22E-06	8.68E-06		
	NIST	-6.16E-07	7.96E-06			1.27E-05	1.03E-05	3.51E-06	1.39E-05	-7.11E-07	1.86E-05	-5.27E-06	1.56E-05
	PTB	-1.33E-05	1.05E-05	-1.27E-05	1.03E-05			-9.15E-06	1.49E-05	-1.34E-05	1.93E-05	-1.79E-05	1.64E-05
9x10^{-4}	NPL	-4.13E-06	1.10E-05	-3.51E-06	1.39E-05	9.15E-06	1.49E-05			-4.23E-06	2.15E-05	-8.78E-06	1.89E-05
	NPLI	9.54E-08	1.40E-05	7.11E-07	1.86E-05	1.34E-05	1.93E-05	4.23E-06	2.15E-05			-4.55E-06	2.26E-05
	KRISS	4.65E-06	1.21E-05	5.27E-06	1.56E-05	1.79E-05	1.64E-05	8.78E-06	1.89E-05	4.55E-06	2.26E-05		

Table 13b. Summary of degree of equivalence to reference value and pair-wise degree of equivalence between the participants, expressed as $d_j/U(d_j)$ or $d_{jj'}/U(d_{jj'})$. Shaded cells indicate results where $|d_j|$ exceeds $U(d_j)$ or $|d_{jj'}|$ exceeds $U(d_{jj'})$. Fractional difference d_j/p_R or $d_{jj'}/p_R$ given at same points.

				NMI$_{j'}$ = NIST		NMI$_{j'}$ = PTB		NMI$_{j'}$ = NPL		NMI$_{j'}$ = NPLI		NMI$_{j'}$ = KRISS	
P_T / Pa	NMI$_j$	d_j/p_R	$d_j / U(d_j)$	$d_{jj'}/p_R$	$d_{jj'} / U(d_{jj'})$	$d_{jj'}/p_R$	$d_{jj'} / U(d_{jj'})$	$d_{jj'}/p_R$	$d_{jj'} / U(d_{jj'})$	$d_{jj'}/p_R$	$d_{jj'} / U(d_{jj'})$	$d_{jj'}/p_R$	$d_{jj'} / U(d_{jj'})$
	NIST	-0.0110	-0.431			0.0163	0.447	-0.0236	-0.489	-0.0066	-0.133	-0.0138	-0.285
	PTB	-0.0273	-0.804	-0.0163	-0.447			-0.0399	-0.789	-0.0229	-0.443	-0.0301	-0.595
$3x10^{-6}$	NPL	0.0126	0.355	0.0236	0.489	0.0399	0.789			0.0171	0.282	0.0099	0.166
	NPLI	-0.0044	-0.122	0.0066	0.133	0.0229	0.443	-0.0171	-0.282			-0.0072	-0.119
	KRISS	0.0028	0.078	0.0138	0.285	0.0301	0.595	-0.0099	-0.166	0.0072	0.119		
	NIST	-0.0029	-0.157			0.0236	0.899	-0.0156	-0.443	0.0001	0.003	0.0040	0.118
	PTB	-0.0265	-1.059	-0.0236	-0.899			-0.0392	-1.050	-0.0235	-0.607	-0.0196	-0.539
$9x10^{-6}$	NPL	0.0127	0.486	0.0156	0.443	0.0392	1.050			0.0157	0.347	0.0196	0.454
	NPLI	-0.0030	-0.109	-0.0001	-0.003	0.0235	0.607	-0.0157	-0.347			0.0039	0.088
	KRISS	-0.0069	-0.271	-0.0040	-0.118	0.0196	0.539	-0.0196	-0.454	-0.0039	-0.088		
	NIST	0.0011	0.068			0.0270	1.187	-0.0075	-0.242	0.0020	0.059	0.0099	0.322
	PTB	-0.0259	-1.160	-0.0270	-1.187			-0.0345	-1.035	-0.0250	-0.709	-0.0171	-0.518
$3x10^{-5}$	NPL	0.0086	0.365	0.0075	0.242	0.0345	1.035			0.0094	0.230	0.0174	0.444
	NPLI	-0.0009	-0.035	-0.0020	-0.059	0.0250	0.709	-0.0094	-0.230			0.0079	0.194
	KRISS	-0.0088	-0.378	-0.0099	-0.322	0.0171	0.518	-0.0174	-0.444	-0.0079	-0.194		
	NIST	-0.0014	-0.117			0.0268	1.663	-0.0092	-0.413	-0.0055	-0.204	0.0091	0.383
	PTB	-0.0282	-1.720	-0.0268	-1.663			-0.0360	-1.500	-0.0322	-1.144	-0.0177	-0.700
$9x10^{-5}$	NPL	0.0078	0.449	0.0092	0.413	0.0360	1.500			0.0037	0.117	0.0183	0.617
	NPLI	0.0041	0.200	0.0055	0.204	0.0322	1.144	-0.0037	-0.117			0.0145	0.439
	KRISS	-0.0105	-0.572	-0.0091	-0.383	0.0177	0.700	-0.0183	-0.617	-0.0145	-0.439		
	NIST	0.0020	0.197			0.0164	1.211	0.0042	0.225	-0.0068	-0.278	0.0106	0.555
	PTB	-0.0144	-1.028	-0.0164	-1.211			-0.0122	-0.602	-0.0232	-0.907	-0.0058	-0.280
$3x10^{-4}$	NPL	-0.0022	-0.148	-0.0042	-0.225	0.0122	0.602			-0.0110	-0.383	0.0064	0.264
	NPLI	0.0088	0.476	0.0068	0.278	0.0232	0.907	0.0110	0.383			0.0174	0.602
	KRISS	-0.0086	-0.572	-0.0106	-0.555	0.0058	0.280	-0.0064	-0.264	-0.0174	-0.602		
	NIST	-0.0007	-0.077			0.0141	1.230	0.0039	0.252	-0.0008	-0.038	-0.0059	-0.338
	PTB	-0.0148	-1.260	-0.0141	-1.230			-0.0102	-0.614	-0.0149	-0.693	-0.0199	-1.090
$9x10^{-4}$	NPL	-0.0046	-0.375	-0.0039	-0.252	0.0102	0.614			-0.0047	-0.197	-0.0098	-0.464
	NPLI	0.0001	0.007	0.0008	0.038	0.0149	0.693	0.0047	0.197			-0.0051	-0.202
	KRISS	0.0052	0.385	0.0059	0.338	0.0199	1.090	0.0098	0.464	0.0051	0.202		

(d_j, $U(d_j)$, $d_{jj'}$, $U(d_{jj'})$) in units of Pa; Table 13b lists the parameters as a relative difference (d_j/p_R, $d_{jj'}/p_R$) or as a difference divided by the expanded uncertainty ($d_j/U(d_j)$, $d_{jj'}/U(d_{jj'})$). In both tables, shaded cells indicate results where there is a lack of degree of equivalence at the k=2 level.

The pair-wise differences and their uncertainties show equivalence between primary standards of NIST, NPL, NPLI, and KRISS at all pressures. PTB shows equivalence to all NMIs at 3×10^{-6} Pa. The following are the 9 pairs of NMIs (out of 120 total pairs) that show lack of equivalence at other pressures:

9×10^{-6} Pa: PTB to NPL
3×10^{-5} Pa: PTB to NIST, PTB to NPL
9×10^{-5} Pa: PTB to NIST, PTB to NPL, PTB to NPLI
3×10^{-4} Pa: PTB to NIST
9×10^{-4} Pa: PTB to NIST, PTB to KRISS

7.4 Discussion of PTB results

As previously mentioned in Sec. 2.2, PTB identified some errors in their CE3/FM3 primary standard, where the virtual leak inside the working volume of FM3 caused the most significant deviation of the measured value from the true physical value which was the conductance of the element generating the flow to the CE3 system. Having redressed the errors and re-measured changed parameters at PTB, the bilateral follow-on comparison CCM.P-K3.1 of this KC is presently under way. Results of the comparison will determine if the corrective actions were successful.

Underestimated uncertainties could be another possible reason for non-equivalence. Table 6 shows that the Type B uncertainties of PTB are the lowest of the five participants. A small uncertainty together with an error in the apparatus more easily leads to a non-equivalence than for the case of a standard with a relatively high uncertainty. Since the CE3/FM3 standard was very new at the time of the comparison and no long-term experience existed, it could be that some contributions were underestimated. A re-examination of the contributions in 2005, however, did not reveal a significant change of the uncertainties estimated for the comparison and PTB still had reason to believe in the uncertainties. For example, by the use of cryo-condensation pumps with practically no back-streaming, and by the use of a conductance in the flowmeter that allows a drift measurement between the reference and working volumes, there are reasons to believe that the uncertainties can be lower than in similar standards. The uncertainties will be re-examined again in the context of the CCM.P-K3.1.

8. Conclusions

Comparisons of vacuum standards are challenging because the instability of the available transfer standards is often higher than the uncertainty of the primary standards that are being

compared. In this comparison, the standard uncertainty of the transfer standards due to long-term shifts was characterized by the relative standard deviation of four calibrations at the pilot laboratory and the two calibrations at PTB (corrected for small sample size), between which there were multiple shipping events. This component of the relative standard uncertainty for the two SRGs was 0.58 % and 1.05 %; for the ion gauge it ranged from 0.26 % to 1.88 % (after normalizing to the shifts at 9×10^{-4} Pa). These values are typical for gauges of this type. The metal-enclosed "Stabil-Ion" gauge proved to be more robust than the glass-envelope type ion gauges (two of which failed during shipment), and was more stable than the one glass-envelope ion gauge calibrated by most of the participants. The relative standard deviation of the four calibrations at the pilot laboratory for BA-16, uncorrected for pressure independent shifts, was 13.9 % to 14.4 %. It is recommended that future comparisons in this pressure range consider using the "Stabil-Ion" gauge in preference to glass envelope gauges. The pressure-independent shift common to ion gauges was corrected by normalization to the SRG results at 9×10^{-4} Pa. This reduced the long-term shift uncertainty of the ion gauge at the higher pressures of the comparison.

Within the limitation imposed by the available transfer standards, this comparison provides useful information on the agreement of the pressure standards of the NMIs over the pressure range of the comparison. One of the participants discovered technical errors in the operation of their vacuum standard that affected all their data, and their result was excluded in the calculation of the KCRV. The KCRV was defined using the arithmetic (unweighted) mean of the remaining four participants. The resulting value was shifted by a scaling factor, chosen such that the KCRV numerically equaled the target pressure. The same scaling factor was used to determine the corrected mean gauge pressure readings of the participants. Such a scaling has no effect on the degree of equivalence of the participants to the KCRV, nor does it have any effect on the degree of equivalence between participants. The four NMIs used in the definition of the KCRV showed equivalence to the KCRV and each other over the full range of pressures at the k=2 level. The NMI not included in calculating the KCRV was equivalent to the KCRV at 3×10^{-6} Pa only (and only marginally non-equivalent at 9×10^{-6} Pa and 3×10^{-4} Pa), and showed lack of equivalence to one or more NMIs at 9×10^{-6} Pa to 9×10^{-4} Pa. The one NMI which used the series expansion method for its primary standard was equivalent to three NMIs using the dynamic expansion method for their primary standards. Within the uncertainty limits imposed by the transfer standards, there is no apparent bias between the two methods.

Appendix A. Proposal for Key Comparison Reference Value and Degrees of Equivalence

There are two issues to address in the choice of the KCRV. The first is whether the data from all participants should be included in its definition; the second is what method to use in combining that subset of participants to form the KCRV.

When the dispersion of the participants' results is larger than expected based on the associated measurement uncertainties, the choice of the KCRV becomes problematic. One method for handling such a situation is to exclude the result from one or more participants in determining the KCRV; with the KCRV so defined, there is more consistency with the results of the reduced number of participants. A number of publications recently have addressed procedures for determining a "consistent subset" (see [19]). Some of the shortcomings of the procedures have been set forth in [20]. Fundamentally, it is preferable only to exclude results for substantive reasons rather than based on a statistical test. Such statistical tests may exclude apparent outliers that are in fact closer to the true value of the SI; in addition, a set of disperse results may indicate that there is unaccounted for uncertainty in the measurement results that must be estimated and included in the uncertainty of the KCRV.

In the present comparison, PTB's calibration ratios measured for the SRGs and ion gauge are consistently lower than the lowest value from the other NMIs. In 2008 PTB found a discrepancy between their continuous expansion system used in this comparison (CE3) and their static expansion system; that disagreement was larger than their combined uncertainties. Subsequently they found technical errors in CE3 that they have corrected, and now have good agreement between the two systems. They have reason to believe that those errors existed at the time of the data collection for this comparison. This is a substantive reason for removing the PTB result from the KCRV, which has been agreed to by PTB.

The data from the remaining four participants (NIST, NPL, NPLI, and KRISS) are all used in calculating the KCRV. The model for the KCRV and the resulting degrees of equivalence (DoE) is based on the Supra Bayesian analysis described in [21]. In this analysis, the DoE are regarded as laboratory biases and are included in the Bayesian "likelihood function", along with the pilot lab's likelihood function for data on x_j (which in this case are the mean gauge pressure readings from the participants). The x_j are all estimates of X, whose posterior distribution will be used to estimate the KCRV. Bayes theorem is applied by using prior distributions for the values of X and the DoE that are "non-informative", meaning nothing is assumed to be known about the laboratory biases or the KCRV prior to the analysis. This is done to keep the analysis as objective as possible.

The result of the model is identical to the arithmetic mean that would be derived from the frequentist analysis assuming that the laboratories all have the same level of uncertainty. We state the result here and refer the reader to [21] for more details. We first determine the uncorrected reference pressure as p_{RU} as the mean of the posterior distribution:

$$p_{RU} = \frac{1}{n_R}\sum_{j=1}^{n_R} p_{jU} \ . \tag{35}$$

The number of labs used in determining the reference value, n_R, is 4, and does not include PTB. The uncertainty of p_{RU} is given by the standard deviation of the posterior distribution:

$$u(p_{RU}) = \frac{1}{n_R}\left(\sum_{j=1}^{n_R} u_c^2(p_{jU})\right)^{1/2} \ . \tag{36}$$

We can now determine the scaling factor, f_C, which sets the reference pressure numerically equal to the target pressure:

$$f_C = \frac{P_T}{p_{RU}} \ . \tag{37}$$

Using eq. (37) with eqs. (8) and (25) we then have the reference pressure and its uncertainty:

$$\begin{aligned} p_R &= \frac{1}{n_R}\sum_{j=1}^{n_R} p_j = \frac{f_C}{n_R}\sum_{j=1}^{n_R} p_{jU} \\ u(p_R) &= \frac{1}{n_R}\left(\sum_{j=1}^{n_R} u_c^2(p_j)\right)^{1/2} \end{aligned} \ . \tag{38}$$

The scaling factors and reference pressure uncertainties for the target pressures are listed in Table A1.

The degree of equivalence is defined as the difference of the laboratory result from the reference value along with the uncertainty of the difference. In the Supra Bayesian model, the difference, d_j is the posterior mean of the laboratory bias, given by

$$d_j = p_j - p_R \ . \tag{39}$$

For all NMIs except PTB, the uncertainty in d_j is given by the standard deviation of the posterior distribution from the Bayesian analysis:

$$u(d_j) = \left(\left(1 - 2/n_R\right)u_c^2(p_j) + u^2(p_R)\right)^{1/2} \ . \tag{40}$$

As results from PTB were not used in determining the reference value, the uncertainty for them is [22]:

$$u(d_{\mathrm{PTB}}) = \left(u_c^2(p_{\mathrm{PTB}}) + u^2(p_R)\right)^{1/2} \ . \tag{41}$$

Table A1. Uncorrected reference pressure, p_{RU}, scaling factor, f_C, reference pressure (KCRV), p_R, and standard uncertainty in reference pressure, $u(p_R)$ as a function of target pressure.

P_T / Pa	p_{RU} / Pa	f_C	p_R / Pa	$u(p_R)$ / Pa	$u(p_R)/p_R$
$3\text{x}10^{-6}$	2.917E-06	1.0285	3.00E-06	2.903E-08	0.00968
$9\text{x}10^{-6}$	8.726E-06	1.0314	9.00E-06	6.374E-08	0.00708
$3\text{x}10^{-5}$	2.928E-05	1.0245	3.00E-05	1.923E-07	0.00641
$9\text{x}10^{-5}$	8.833E-05	1.0189	9.00E-05	4.492E-07	0.00499
$3\text{x}10^{-4}$	2.976E-04	1.0079	3.00E-04	1.293E-06	0.00431
$9\text{x}10^{-4}$	9.024E-04	0.9974	9.00E-04	3.314E-06	0.00368

Equivalence to the KCRV is evaluated by comparing the difference in eq. (39) to the expanded (k=2) uncertainty in the difference. There is equivalence if:

$$\frac{|d_j|}{U(d_j)} \le 1.0 \quad , \qquad U(d_j) = 2u(d_j) \tag{42}$$

Degrees of equivalence between participants are given by pair-wise differences in the deviation from the reference pressure and the associated uncertainty:

$$d_{jj'} = d_j - d_{j'} = (p_j - p_R) - (p_{j'} - p_R) = p_j - p_{j'} \ . \tag{43}$$

The standard uncertainty in pair-wise differences between NMI j and NMI j' is given by:

$$u(d_{jj'}) = \left(u_c^2(p_j) + u_c^2(p_{j'})\right)^{1/2} \ . \tag{44}$$

There is equivalence between pairs of participants if:

$$\frac{|d_{jj'}|}{U(d_{jj'})} \le 1.0 \quad , \qquad U(d_{jj'}) = 2u(d_{jj'}) \tag{45}$$

Note that neither the pair-wise differences nor their uncertainties depend on the definition of p_R or its uncertainty.

Acknowledgements

The NIST authors gratefully acknowledge the contribution of J.P. Looney of the NIST Pressure and Vacuum Group who organized the key comparison, co-wrote the protocol, and assisted with the NIST calibrations. W.F. Guthrie of the Statistical Engineering Division at NIST provided extremely valuable guidance and insight on the statistical treatment of the calibration data and is acknowledged for that effort. NIST Group member D.R. Defibaugh assisted with the NIST calibrations. P. Mohan of NPLI acknowledges the contribution of his colleague Harish Kumar in upgrading the NPLI standard from the diffusion pump version to the turbomolecular drag pump version used in the comparison.

References

1. Comité International des Poids et Mesures (CIPM), Mutual recognition of national measurement standards and of calibration and measurement certificates issued by national metrology institutes, Paris (1999), pp. 45.

2. Dittmann, S., "High vacuum standard and its use", NIST Special Publication SP 250-34 (1989).

3. Jousten, K., Menzer, H., Wandrey, D., and Niepraschk, R., "New, fully automated, primary standard for generating vacuum pressures between 10^{-10} and 3×10^{-2} Pa with respect to residual pressure", Metrologia 36 (1999) 493-497.

4. Jousten, K., Menzer, H., and Niepraschk, R., "A new fully automated gas flowmeter at the PTB for flow rates between 10^{-13} mol/s and 10^{-6} mol/s", Metrologia, 39 (2002) 519-529.

5. Redgrave, F.J., Forbes, A.B., and Harris, P.M., "A discussion of methods for the estimation of volumetric ratios determined by multiple expansions", Vacuum 53 (1999) 159-162.

6. Mohan, P., "Vacuum gauge calibration at the NPL (India) using orifice flow method", Vacuum 51 (1998) 69-74.

7. Mohan, P., and Gupta, A.C., "Use of a calibrated leak for the calibration of vacuum gauges", Vacuum 48 (1997) 515-519.

8. Hong, S.S., Shin, Y.H., and Chung, K.H., "Measurement uncertainties for vacuum standards at Korea Research Institute of Standards and Science", J. Vac. Sci. Technol. A 24(5) (2006) 1831-1838.

9. Filippelli, A.R., and Abbott, P.J., "Long term stability of Bayard-Alpert ionization gauge performance", J. Vac. Sci. Technol. A (13) (1995) 2582-2586.

10. Chang, R.F., and Abbott, P.J., "Factors affecting the accommodation coefficient of the spinning rotor gauge", J. Vac. Sci. Technol. A 25(6) (2007) 1567-1576.

11. Jousten, K., Filippelli, A.R., Tilford, C.R., and Redgrave, F.J., "Comparison of the standards for high and ultrahigh vacuum at three national standards laboratories", J. Vac. Sci. Technol. A 15(4) (1997) 2395-2406.

12. Zhang, N.F., "The uncertainty associated with the weighted mean of measurement data", Metrologia 43 (2006) 195-204.

13. Miiller, A.P., Bergoglio, M., Bignell, N., Fen, K.M.K., Hong, S.S., Jousten, K., Mohan, P., Redgrave, F.J., and Sardi, M., "Final report on key comparison CCM.P-K4 in absolute pressure from 1 to 1000 Pa", Metrologia 39 (2002) Tech. Suppl. 07001.

14. Miiller, A.P., Cignolo, G., Fitzgerald, M.P., and Perkin, M.P., "Final report of key comparison CCM.P-K5 in differential pressure from 1 Pa to 1000 Pa", Metrologia 39 (2002) Tech. Suppl. 07002.

15. Jousten, K., Bergoglio, M., Calcatelli, A., Durocher, J.N., Greenwood, J., Kungi, R., Legras, J.C., Matilla, C., and Setina, J., "Final report on the regional key comparison Euromet.M.P-K1.b in the pressure range from 3×10^{-4} Pa to 0.9 Pa", Metrologia 42 (2005) Tech. Suppl. 07001.

16. Taylor, B.N., and Kuyatt, C.E., "Guidelines for evaluating and expressing the Uncertainty of NIST measurement results", NIST Technical Note 1297 (1994).

17. Kacker, R., and Jones, A., "On use of Bayesian statistics to make the 'Guide to the expression of uncertainty in measurement' consistent", Metrologia 40 (2003) 235-248.

18. Abbott, P.J., Looney, J.P., and Mohan, P., "The effect of ambient temperature on the sensitivity of hot-cathode ionization gauges," Vacuum 77 (2005) 217-222.

19. Cox, M.G., "The evaluation of key comparison data: determining the largest consistent subset", Metrologia 44 (2007) 187-200.

20. Toman, B., and Possolo, A., "Laboratory effects models for interlaboratory comparisons", Accred Qual Assur, DOI 10.1007/s00769-009-0547-2 (2009) online.

21. Toman, B., "Statistical interpretation of key comparison degrees of equivalence based on distribution of belief", Metrologia 44 (2007) L14-L17.

22. Ratel, G., "Evaluating the uncertainty of degree of equivalence", Metrologia 42 (2005) 140-144.